# Blind Multiuser Detection: A Subspace Approach

Xiaodong Wang and H. Vincent Poor, *Fellow, IEEE*

***Abstract*— A new multiuser detection scheme based on signal subspace estimation is proposed. It is shown that under this scheme, both the decorrelating detector and the linear minimum-mean-square-error (MMSE) detector can be obtained blindly, i.e., they can be estimated from the received signal with the prior knowledge of only the signature waveform and timing of the user of interest. The consistency and asymptotic variance of the estimates of the two linear detectors are examined. A blind adaptive implementation based on a signal subspace tracking algorithm is also developed. It is seen that compared with the previous minimum-output-energy blind adaptive multiuser detector, the proposed subspace-based blind adaptive detector offers lower computational complexity, better performance, and robustness against signature waveform mismatch. Two extensions are made within the framework of signal subspace estimation. First, a blind adaptive method is developed for estimating the effective user signature waveform in the multipath channel. Secondly, a multiuser detection scheme using spatial diversity in the form of an antenna array is considered. A blind adaptive technique for estimating the array response for diversity combining is proposed. It is seen that under the proposed subspace approach, blind adaptive channel estimation and blind adaptive array response estimation can be integrated with blind adaptive multiuser detection, with little attendant increase in complexity.**

***Index Terms*— Array response estimation, blind adaptation, channel estimation, linear multiuser detection, subspace tracking.**

## I. Introduction

CODE-division multiple-access (CDMA) implemented with direct-sequence spread-spectrum (DS–SS) modulation is emerging as a popular multiple-access technology for personal, cellular, and satellite communication services [13], [37]. Multiuser detection techniques can substantially increase the capacity of CDMA systems. Over the past decade, a significant amount of research has addressed various multiuser detection schemes [35]. Considerable recent attention has been focused on adaptive multiuser detection [8]. For example, methods for adapting the decorrelating, or zero-forcing, linear detector that require the transmission of training sequences during adaptation have been proposed in [4], [21], and [22]. An alternative linear detector, the minimum-mean-square-error (MMSE) detector, however, can be adapted either through the use of training sequences [1], [17], [20], [28], or in the blind mode, i.e., with the prior knowledge of only the signature waveform and timing of the user of interest [7], [26]. Blind adaptation schemes are especially attractive for the downlinks of CDMA systems, since in a dynamic environment, it is very difficult for a mobile user to obtain accurate information on other active users in the channel, such as their signature waveforms; and the frequent use of training sequence is certainly a waste of channel bandwidth.

In this paper, we propose a new blind multiuser detection scheme which is based on signal subspace estimation. Subspace-based high-resolution methods play an important role in sensor array processing, spectrum analysis, and general parameter estimation [34]. Several recent works have addressed the use of subspaced-based methods for delay estimation [2], [31] and channel estimation [2], [14] in CDMA systems.

The contribution of this work is threefold. First of all, we show that based on signal subspace estimation, both the decorrelating detector and the linear MMSE detector can be obtained blindly, i.e., they can be estimated from the received signal with the prior knowledge of only the signature waveform and timing of the user of interest. The consistency and the asymptotic variance of the estimates of the two subspace-based linear detectors are examined. A blind adaptive implementation based on a signal subspace tracking algorithm is also developed. It is seen that compared with the previous minimum-output-energy (MOE) blind adaptive detector [7], this subspace-based blind adaptive detector offers lower computational complexity ($O(NK)$, where $N$ is the processing gain, $K$ is the number of active users in the channel.) and better performance in terms of the steady-state signal-to-interference ratio (SIR). Moreover, the proposed detector is made robust against signature waveform mismatch through nulling out the noise subspace component of the mismatched signature waveform, and through adaptive estimation of the effective signature waveform.

The second contribution of this work is the development of a blind adaptive method for estimating the effective signature waveform in the multipath channel. Under certain conditions, the problem of identifying the multipath channel gains is equivalent to fitting the estimated signal subspace with the subspace spanned by the known nominal signature waveforms. We show that this subspace fitting problem can in turn be transformed into an unconstrained minimization problem whose local minimum is unique, and thus can be solved by the method of steepest descent. It is seen that by employing this blind adaptive algorithm for joint channel estimation and multiuser detection, little performance degradation is incurred when the signal is distorted by the multipath channel.

The third contribution of this work is the extension of the subspace approach to multiuser detection using spatial

Manuscript received January 10, 1997; revised September 4, 1997. This work was supported by the the U.S. Office of Naval Research under Grant N00014-94-1-0115. The material in this paper was presented in part at the 31st Annual Conference on Information Sciences and Systems, The Johns Hopkins University, Baltimore, MD, March 19–21, 1997.

The authors are with the Department of Electrical Engineering, Princeton University, Princeton, NJ 08544 USA.

Publisher Item Identifier S 0018-9448(98)00840-2.

diversity in the form of an antenna array. Here the key issue is to estimate the array response to the desired user's signal for diversity combining. Since the number of users in CDMA channels far exceeds the number of antenna elements, the conventional subspace-based estimation algorithms, such as MUSIC, ESPRIT, etc., cannot be applied. We propose a blind adaptive estimation method based on the output of a bank of linear multiuser detectors at the antenna array. It is seen that this algorithm has a low computational complexity, while it is capable of closely tracking the array response to the desired user's signal.

The rest of the paper is organized as follows. In Section II, the signal model is introduced. In Section III, two subspace-based linear multiuser detectors, namely, the decorrelating detector and the linear MMSE detector, are developed. In Section IV, a blind adaptive implementation of the subspace-based linear MMSE detector, which is based on a signal subspace tracking algorithm, is developed. In Section V, the performance of the proposed subspace-based linear detectors under signature waveform mismatch is considered; and a blind adaptive method for estimating the effective signature waveform in the multipath channel is developed. In Section VI, a multiuser detection scheme using spatial diversity in the form of an antenna array is considered; and a blind adaptive technique for estimating the array response for diversity combining is proposed. Section VII contains the conclusion.

## II. Signal Model

Consider a baseband digital direct sequence (DS) CDMA network of $K$ users. The received signal can be modeled as

$$r(t) = S(t) + \sigma n(t) \tag{1}$$

where $n(t)$ is white Gaussian noise with unit power spectral density, and $S(t)$ is the superposition of the data signals of the $K$ users, given by

$$S(t) = \sum_{k=1}^{K} A_k \sum_{i=-M}^{M} b_k(i) s_k(t - iT - \tau_k) \tag{2}$$

where $2M+1$ is the number of data symbols per user per frame, $T$ is the symbol interval, and where $A_k, \tau_k, \{b_k(i); i = 0, \pm 1, \cdots, \pm M\}$ and $\{s_k(t); 0 \le t \le T\}$ denote, respectively, the received amplitude, delay, symbol stream, and normalized signaling waveform of the $k$th user. It is assumed that $s_k(t)$ is supported only on the interval $[0, T]$ and has unit energy, and that $\{b_k(i)\}$ is a collection of independent equiprobable $\pm 1$ random variables. For the direct-sequence spread-spectrum (DS-SS) multiple-access format, the user signaling waveforms are of the form

$$s_k(t) = \sum_{j=0}^{N-1} \beta_j^k \psi(t - jT_c), \qquad t \in [0, T] \tag{3}$$

where $N$ is the processing gain; $(\beta_0^k, \beta_1^k, \cdots, \beta_{N-1}^k)$ is a signature sequence of $\pm 1$'s assigned to the $k$th user; and $\psi$ is a normalized chip waveform of duration $T_c$, where $NT_c = T$.

In this paper, we restrict our attention to the synchronous case of model (2), in which $\tau_1 = \tau_2 = \cdots = \tau_K = 0$. It is then sufficient to consider the received signal during one symbol interval, and the received signal model becomes

$$r(t) = \sum_{k=1}^{K} A_k b_k s_k(t) + \sigma n(t), \qquad t \in [0, T]. \tag{4}$$

One simple suboptimal way to treat the asynchronous system is the "one-shot" approach, in which a particular transmitted data bit is estimated based on only the received signal within the symbol interval corresponding to that data bit. An asynchronous system of $K$ users can then be viewed as equivalent to a synchronous system with $2K-1$ users [17], and the results of this paper thus apply in this context as well. Alternatively, an asynchronous CDMA system is a special case of the more general dispersive CDMA system in which the channel introduces intersymbol interference (ISI), in addition to the multiple-access interference (MAI). The subspace-based techniques considered in this paper can also be extended to such a dispersive CDMA system for blind joint suppression of both MAI and ISI [38].

Consider the synchronous model (4). At the receiver, chip-matched filtering followed by chip rate sampling yields an $N$-vector of chip-matched filter output samples within a symbol interval $T$

$$\boldsymbol{r} = \sum_{k=1}^{K} A_k b_k \boldsymbol{s}_k + \sigma \boldsymbol{n} \tag{5}$$

where

$$\boldsymbol{s}_k = (1/\sqrt{N})[\beta_0^k \ \beta_1^k \cdots \beta_{N-1}^k]^T$$

is the normalized signature waveform vector of the $k$th user, and $\boldsymbol{n}$ is a white Gaussian noise vector with mean $\mathbf{0}$ and covariance matrix $\boldsymbol{I}_N$ ($\boldsymbol{I}_N$ denotes the $N \times N$ indentity matrix). Thus we can restrict attention to the discrete-time model (5).

## III. Subspace-Based Blind Linear Multiuser Detectors

### A. Subspace Concept

For convenience and without loss of generality, we assume that the signature waveforms $\{\boldsymbol{s}_k\}_{k=1}^K$ of the $K$ users are linearly independent. Denote $\boldsymbol{S} \triangleq [\boldsymbol{s}_1 \ \ \boldsymbol{s}_2 \cdots \boldsymbol{s}_K]$ and $\boldsymbol{A} \triangleq \mathrm{diag}\,(A_1^2, \cdots, A_K^2)$. The autocorrelation matrix of the received signal $\boldsymbol{r}$ is then given by

$$\boldsymbol{C} \triangleq E\{\boldsymbol{r}\,\boldsymbol{r}^T\} = \sum_{k=1}^{K} A_k^2 \boldsymbol{s}_k \boldsymbol{s}_k^T + \sigma^2 \boldsymbol{I}_N = \boldsymbol{SAS}^T + \sigma^2 \boldsymbol{I}_N. \tag{6}$$

By performing an eigendecomposition of the matrix $\boldsymbol{C}$, we get

$$\boldsymbol{C} = \boldsymbol{U\Lambda U}^T = [\boldsymbol{U}_s \quad \boldsymbol{U}_n] \begin{bmatrix} \boldsymbol{\Lambda}_s & \\ & \boldsymbol{\Lambda}_n \end{bmatrix} \begin{bmatrix} \boldsymbol{U}_s^T \\ \boldsymbol{U}_n^T \end{bmatrix} \tag{7}$$

where

$$\boldsymbol{U} = [\boldsymbol{U}_s \ \boldsymbol{U}_n], \boldsymbol{\Lambda} = \mathrm{diag}\,(\boldsymbol{\Lambda}_s, \boldsymbol{\Lambda}_n); \boldsymbol{\Lambda}_s = \mathrm{diag}\,(\lambda_1, \cdots, \lambda_K)$$

contains the $K$ largest eigenvalues of $\boldsymbol{C}$ in descending order and $\boldsymbol{U}_s = [\boldsymbol{u}_1 \cdots \boldsymbol{u}_K]$ contains the corresponding orthonormal eigenvectors; $\boldsymbol{\Lambda}_n = \sigma^2 \boldsymbol{I}_{N-K}$ and $\boldsymbol{U}_n = [\boldsymbol{u}_{K+1} \cdots \boldsymbol{u}_N]$

contains the $N-K$ orthonormal eigenvectors that correspond to the eigenvalue $\sigma^2$. It is easy to see that range$(\boldsymbol{S}) =$ range$(\boldsymbol{U}_s)$. The range space of $\boldsymbol{U}_s$ is called the *signal subspace* and its orthogonal complement, the *noise subspace*, is spanned by $\boldsymbol{U}_n$. Define the $N \times N$ diagonal matrix $\boldsymbol{\Lambda}_0 \triangleq \boldsymbol{\Lambda} - \sigma^2 \boldsymbol{I}_N = \text{diag}(\lambda_1 - \sigma^2, \cdots, \lambda_K - \sigma^2, 0, \cdots, 0)$. From (6) and (7) we obtain

$$\boldsymbol{S}\boldsymbol{A}\boldsymbol{S}^T = \boldsymbol{U}_s(\boldsymbol{\Lambda}_s - \sigma^2\boldsymbol{I}_K)\boldsymbol{U}_s^T = \boldsymbol{U}\boldsymbol{\Lambda}_0\boldsymbol{U}^T. \tag{8}$$

A linear multiuser detector for demodulating the $k$th user's data bit in (5) is in the form of a correlator followed by a hard limiter

$$\hat{b}_k = \text{sgn}(\boldsymbol{w}_k^T \boldsymbol{r}) \tag{9}$$

where $\boldsymbol{w}_k \in \mathcal{R}^N$. Next we derive expressions for two linear multiuser detectors, namely, the decorrelating detector and the linear MMSE detector, in terms of the signal subspace parameters ($\boldsymbol{U}_s$, $\boldsymbol{\Lambda}_s$, and $\sigma$).

### B. Decorrelating Detector

The correlation matrix of the signature waveforms is defined as $\boldsymbol{R} \triangleq \boldsymbol{S}^T\boldsymbol{S}$. Since rank $(\boldsymbol{S}) = K$, it follows that $\boldsymbol{R}$ is invertible. Henceforth let user 1 be the user of interest. The decorrelating detector [16] is designed to completely eliminate the multiple-access interference (MAI) caused by other users, at the expense of enhancing the ambient noise. It has the form of (9) with the weight vector $\boldsymbol{w}_1 = \boldsymbol{d}_1$ given by

$$\boldsymbol{d}_1 = \sum_{k=1}^{K} [\boldsymbol{R}^{-1}]_{1k} \boldsymbol{s}_k \tag{10}$$

where $[\boldsymbol{R}^{-1}]_{ij}$ denotes the $(i,j)$th element of the matrix $\boldsymbol{R}^{-1}$. The weight vector in (10) is characterized by the following results.

*Lemma 1:* The decorrelating detector $\boldsymbol{d}_1$ in (10) is the unique signal $\boldsymbol{d} \in$ range $(\boldsymbol{U}_s)$, such that $\boldsymbol{d}^T\boldsymbol{s}_1 = 1$, and $\boldsymbol{d}^T\boldsymbol{s}_k = 0$, for $k = 2, \cdots, K$.

*Proof:* Since rank $(\boldsymbol{U}_s) = K$, the vector $\boldsymbol{d}$ that satisfies the above conditions exists and is unique. It is seen from (10) that $\boldsymbol{d}_1 \in$ range $(\boldsymbol{S}) =$ range $(\boldsymbol{U}_s)$. Moreover

$$\begin{aligned} \boldsymbol{d}_1^T\boldsymbol{s}_k &= \sum_{i=1}^{K} [\boldsymbol{R}^{-1}]_{1i} \boldsymbol{s}_i^T \boldsymbol{s}_k = \sum_{i=1}^{K} [\boldsymbol{R}^{-1}]_{1i} [\boldsymbol{R}]_{ik} \\ &= [\boldsymbol{R}^{-1}\boldsymbol{R}]_{1k} = \begin{cases} 1, & k = 1 \\ 0, & k = 2, \cdots, K. \end{cases} \end{aligned} \tag{11}$$

Therefore, $\boldsymbol{d}_1 = \boldsymbol{d}$. □

*Lemma 2:* The decorrelating detector $\boldsymbol{d}_1$ in (10) is the unique signal $\boldsymbol{d} \in$ range $(\boldsymbol{U}_s)$ that minimizes

$$\varphi(\boldsymbol{d}) \triangleq E\left\{\left[\boldsymbol{d}^T\left(\sum_{k=1}^{K} A_k b_k \boldsymbol{s}_k\right)\right]^2\right\}$$

subject to $\boldsymbol{d}^T\boldsymbol{s}_1 = 1$.

*Proof:* Since

$$\begin{aligned} \varphi(\boldsymbol{d}) &= \boldsymbol{d}^T E\left\{\left(\sum_{k=1}^{K} A_k b_k \boldsymbol{s}_k\right)\left(\sum_{k=1}^{K} A_k b_k \boldsymbol{s}_k\right)^T\right\}\boldsymbol{d} \\ &= \boldsymbol{d}^T\left(\sum_{k=1}^{K} A_k^2 \boldsymbol{s}_k \boldsymbol{s}_k^T\right)\boldsymbol{d} \\ &= A_1^2(\boldsymbol{d}^T\boldsymbol{s}_1)^2 + \sum_{k=2}^{K} A_k^2(\boldsymbol{d}^T\boldsymbol{s}_k)^2 \\ &= A_1^2 + \sum_{k=2}^{K} A_k^2(\boldsymbol{d}^T\boldsymbol{s}_k)^2 \end{aligned} \tag{12}$$

it then follows that for $\boldsymbol{d} \in$ range $(\boldsymbol{U}_s) =$ range $(\boldsymbol{S})$, $\varphi(\boldsymbol{d})$ is minimized if and only if $\boldsymbol{d}^T\boldsymbol{s}_k = 0$, for $k = 2, \cdots, K$. By Lemma 1, $\boldsymbol{d}_1 = \boldsymbol{d}$. □

*Proposition 1:* The decorrelating detector $\boldsymbol{d}_1$ in (10) is given in terms of the signal subspace parameters by

$$\boldsymbol{d}_1 = \frac{1}{[\boldsymbol{s}_1^T\boldsymbol{U}_s(\boldsymbol{\Lambda}_s - \sigma^2\boldsymbol{I}_K)^{-1}\boldsymbol{U}_s^T\boldsymbol{s}_1]}\boldsymbol{U}_s(\boldsymbol{\Lambda}_s - \sigma^2\boldsymbol{I}_K)^{-1}\boldsymbol{U}_s^T\boldsymbol{s}_1. \tag{13}$$

*Proof:* A signal $\boldsymbol{d} \in$ range $(\boldsymbol{U}_s)$ if and only if it can be written as $\boldsymbol{d} = \boldsymbol{U}_s\boldsymbol{c}$, for some $\boldsymbol{c} \in \mathcal{R}^K$. Then by Lemma 2, the decorrelating detector $\boldsymbol{d}_1$ has the form $\boldsymbol{d}_1 = \boldsymbol{U}_s\boldsymbol{c}_1$, where

$$\begin{aligned} \boldsymbol{c}_1 &= \arg\min_{\boldsymbol{c}\in\mathcal{R}^K} (\boldsymbol{U}_s\,\boldsymbol{c})^T\left(\sum_{k=1}^{K} A_k^2\boldsymbol{s}_k\boldsymbol{s}_k^T\right)(\boldsymbol{U}_s\,\boldsymbol{c}), \\ &\qquad \text{s.t.} \quad (\boldsymbol{U}_s\,\boldsymbol{c})^T\boldsymbol{s}_1 = 1 \\ &= \arg\min_{\boldsymbol{c}\in\mathcal{R}^K} \boldsymbol{c}^T[\boldsymbol{U}_s^T(\boldsymbol{S}\boldsymbol{A}\boldsymbol{S}^T)\boldsymbol{U}_s]\boldsymbol{c}, \\ &\qquad \text{s.t.} \quad \boldsymbol{c}^T(\boldsymbol{U}_s^T\boldsymbol{s}_1) = 1 \\ &= \arg\min_{\boldsymbol{c}\in\mathcal{R}^K} \boldsymbol{c}^T(\boldsymbol{\Lambda}_s - \sigma^2\boldsymbol{I}_K)\boldsymbol{c}, \\ &\qquad \text{s.t.} \quad \boldsymbol{c}^T(\boldsymbol{U}_s^T\boldsymbol{s}_1) = 1 \end{aligned} \tag{14}$$

where the second equality follows from (6) and the third equality follows from (8). The optimization problem (14) can be solved by the method of Lagrange multipliers. Let

$$\mathcal{L}(\boldsymbol{c}) \triangleq \boldsymbol{c}^T(\boldsymbol{\Lambda}_s - \sigma^2\boldsymbol{I}_K)\boldsymbol{c} - 2\mu[\boldsymbol{c}^T(\boldsymbol{U}_s^T\boldsymbol{s}_1) - 1]. \tag{15}$$

Since the matrix $(\boldsymbol{\Lambda}_s - \sigma^2\boldsymbol{I}_K)$ is positive definite, $\mathcal{L}(\boldsymbol{c})$ is a strictly convex function of $\boldsymbol{c}$. Therefore, the unique global minimum of $\mathcal{L}(\boldsymbol{c})$ is achieved at $\boldsymbol{c}_1$ where $\nabla\mathcal{L}(\boldsymbol{c}_1) = \boldsymbol{0}$, or

$$(\boldsymbol{\Lambda}_s - \sigma^2\boldsymbol{I}_K)\boldsymbol{c}_1 = \mu\boldsymbol{U}_s^T\boldsymbol{s}_1. \tag{16}$$

Therefore, $\boldsymbol{c}_1 = \mu(\boldsymbol{\Lambda}_s - \sigma^2\boldsymbol{I}_K)^{-1}\boldsymbol{U}_s^T\boldsymbol{s}_1$, where $\mu$ is determined from the constraint $(\boldsymbol{U}_s\boldsymbol{c}_1)^T\boldsymbol{s}_1 = 1$, i.e.,

$$\mu = 1/[\boldsymbol{s}_1^T\boldsymbol{U}_s(\boldsymbol{\Lambda}_s - \sigma^2\boldsymbol{I}_K)^{-1}\boldsymbol{U}_s^T\boldsymbol{s}_1].$$

Finally, the decorrelating detector is given by

$$\boldsymbol{d}_1 = \boldsymbol{U}_s\boldsymbol{c}_1 = \mu\boldsymbol{U}_s(\boldsymbol{\Lambda}_s - \sigma^2\boldsymbol{I}_K)^{-1}\boldsymbol{U}_s^T\boldsymbol{s}_1.$$ □

### C. Linear MMSE Detector

The canonical form of the linear minimum mean-square-error (MMSE) multiuser detector [7] of user 1 has the form of (9) with the weight vector $\boldsymbol{w}_1 = \boldsymbol{m}_1$, where $\boldsymbol{m}_1 \in \mathcal{R}^N$ minimizes the MSE, defined as

$$\mathrm{MSE}(\boldsymbol{m}_1) \triangleq E\{(A_1 b_1 - \boldsymbol{m}_1^T \boldsymbol{r})^2\} \tag{17}$$

subject to $\boldsymbol{m}_1^T \boldsymbol{s}_1 = 1$.

*Proposition 2:* The linear MMSE detector $\boldsymbol{m}_1$ is given in terms of the signal subspace parameters by

$$\boldsymbol{m}_1 = \frac{1}{[\boldsymbol{s}_1^T \boldsymbol{U}_s \boldsymbol{\Lambda}_s^{-1} \boldsymbol{U}_s^T \boldsymbol{s}_1]} \boldsymbol{U}_s \boldsymbol{\Lambda}_s^{-1} \boldsymbol{U}_s^T \boldsymbol{s}_1. \tag{18}$$

*Proof:* Using (5) and (17), by the method of Lagrange multipliers, we obtain

$$\begin{aligned}\mathcal{L}(\boldsymbol{m}) &\triangleq \mathrm{MSE}(\boldsymbol{m}) - 2\mu(\boldsymbol{m}^T \boldsymbol{s}_1 - 1)\\ &= \boldsymbol{m}^T E\{\boldsymbol{r}\,\boldsymbol{r}^T\}\boldsymbol{m} - 2A_1 \boldsymbol{m}^T E\{b_1 \boldsymbol{r}\}\\ &\quad + A_1^2 - 2\mu(\boldsymbol{m}^T \boldsymbol{s}_1 - 1)\\ &= \boldsymbol{m}^T \boldsymbol{C} \boldsymbol{m} - 2(A_1^2 + \mu)\boldsymbol{m}^T \boldsymbol{s}_1 + (A_1^2 + 2\mu)\end{aligned} \tag{19}$$

where we have used $E\{\boldsymbol{r}\,\boldsymbol{r}^T\} = \boldsymbol{C}$ and $E\{b_1\,\boldsymbol{r}\} = \boldsymbol{s}_1$. Since $\boldsymbol{C}$ is positive definite, $\mathcal{L}(\boldsymbol{m})$ is a strictly convex function of $\boldsymbol{m}$. Therefore, the linear MMSE detector is obtained by solving for $\boldsymbol{m}_1$ from $\nabla \mathcal{L}(\boldsymbol{m}_1) = \boldsymbol{0}$

$$\begin{aligned}\boldsymbol{m}_1 &= (A_1^2 + \mu)\boldsymbol{C}^{-1}\boldsymbol{s}_1\\ &= (A_1^2 + \mu)(\boldsymbol{U}_s \boldsymbol{\Lambda}_s^{-1} \boldsymbol{U}_s^T)\boldsymbol{s}_1 + (A_1^2 + \mu)\sigma^{-2}(\boldsymbol{U}_n \boldsymbol{U}_n^T)\boldsymbol{s}_1\\ &= (A_1^2 + \mu)\boldsymbol{U}_s \boldsymbol{\Lambda}^{-1} \boldsymbol{U}_s^T \boldsymbol{s}_1\end{aligned} \tag{20}$$

where the second equality follows from the eigendecomposition (7) of $\boldsymbol{C}$, and the third equality follows from the fact that $\boldsymbol{s}_1 \in \mathsf{range}\,(\boldsymbol{U}_s)$ is orthogonal to the noise subspace, i.e., $\boldsymbol{U}_n^T \boldsymbol{s}_1 = \boldsymbol{0}$. Finally, from the constraint that $\boldsymbol{m}_1^T \boldsymbol{s}_1 = 1$, we obtain

$$(A_1^2 + \mu) = 1/[\boldsymbol{s}_1^T \boldsymbol{U}_s \boldsymbol{\Lambda}_s^{-1} \boldsymbol{U}_s^T \boldsymbol{s}_1]. \qquad \square$$

*Remark 1:* Since the decision (9) is invariant to positive scaling, the two linear multiuser detectors given by (13) and (18) can be interpreted as follows. First the received signal $\boldsymbol{r}$ is projected onto the signal subspace to get a $K$-vector $\boldsymbol{y} \triangleq \boldsymbol{U}_s^T \boldsymbol{r}$, which clearly is a sufficient statistic for demodulating the $K$ users' data bits. The signature waveform $\boldsymbol{s}_1$ of the user of interest is also projected onto the signal subspace to obtain $\boldsymbol{p}_1 \triangleq \boldsymbol{U}_s^T \boldsymbol{s}_1$. The projection of the linear multiuser detector in the signal subspace is then a signal $\boldsymbol{c}_1 \in \mathcal{R}^K$ such that the data bit is demodulated as $\hat{b}_1 = \mathrm{sgn}\,(\boldsymbol{c}_1^T \boldsymbol{y})$. According to (13) and (18), the projections of the decorrelating detector and the linear MMSE detector in the signal subspace are given, respectively, by

$$\boldsymbol{c}_1^d = \begin{pmatrix} \frac{1}{\lambda_1 - \sigma^2} & & \\ & \ddots & \\ & & \frac{1}{\lambda_K - \sigma^2} \end{pmatrix} \boldsymbol{p}_1, \tag{21}$$

$$\boldsymbol{c}_1^m = \begin{pmatrix} \frac{1}{\lambda_1} & & \\ & \ddots & \\ & & \frac{1}{\lambda_K} \end{pmatrix} \boldsymbol{p}_1. \tag{22}$$

Therefore, the projection of the linear multiuser detectors in the signal subspace are obtained by projecting the signature waveform of the user of interest onto the signal subspace, followed by scaling the $k$th component of this projection by a factor of $1/(\lambda_k - \sigma^2)$ (decorrelating detector) or $1/\lambda_k$ (MMSE detector). Note that as $\sigma \to 0$, the two linear detectors become identical.

*Remark 2:* Since the autocorrelation matrix $\boldsymbol{C}$, and therefore its eigencomponents, can be estimated from the received signal, from the preceding discussion, we see that both the decorrelating detector and the linear MMSE detector can be estimated from the received signal with the prior knowledge of only the signature waveform and timing of the user of interest, i.e., they both can be obtained *blindly*.

### D. Near–Far Resistance

A commonly used performance measure for a multiuser detector is the asymptotic multiuser efficiency (AME) [16], defined as[1]

$$\eta_1 \triangleq \sup\left\{0 \le r \le 1\colon \lim_{\sigma \to 0} P_1(\sigma)/Q\left(\frac{\sqrt{r}A_1}{\sigma}\right) = 0\right\} \tag{23}$$

which measures the exponential decay rate of the error probability as the background noise approaches zero. A related performance measure, the near–far resistance, is the infimum of AME as the interferers' energies are allowed to vary

$$\overline{\eta}_1 = \inf_{\substack{A_k \ge 0\\ k \ne 1}} \{\eta_1\}. \tag{24}$$

It is well known that both the decorrelating detector [16] and the linear MMSE detector [17] achieve the optimal near–far resistance, given by $\overline{\eta}_1 = 1/[\boldsymbol{R}^{-1}]_{11}$. Although it can be inferred that the two detectors given by (13) and (18) must achieve this optimal near–far resistance, since they are simply different forms of the respective original detectors, in the following we compute their near–far resistance directly. Some results in this section will be used later to derive the AME of the subspace-based linear detectors under the signature waveform mismatch.

Recall that the $N \times N$ diagonal matrix

$$\boldsymbol{\Lambda}_0 \triangleq \mathsf{diag}\,(\lambda_1 - \sigma^2, \cdots, \lambda_K - \sigma^2, 0, \cdots, 0).$$

Define

$$\boldsymbol{\Lambda}_0^\dagger \triangleq \mathsf{diag}\,([\lambda_1 - \sigma^2]^{-1}, \cdots, [\lambda_K - \sigma^2]^{-1}, 0, \cdots, 0).$$

Let the singular value decomposition (SVD) of $\boldsymbol{S} \triangleq [\boldsymbol{s}_1\ \boldsymbol{s}_2 \cdots \boldsymbol{s}_K]$ be

$$\boldsymbol{S} = \boldsymbol{W}\boldsymbol{\Sigma}\boldsymbol{V}^T \tag{25}$$

[1] $P_1(\sigma)$ is the probability of error of the detector $Q(x) \triangleq (1/\sqrt{2\pi}) \int_x^\infty e^{-(x^2/2)}\,dx$.

where the $N \times K$ matrix $\mathbf{\Sigma} = [\sigma_{ij}]$ has $\sigma_{ij} = 0$ for all $i \neq j$, and $\sigma_{11} \geq \sigma_{22} \geq \cdots \geq \sigma_{KK}$. The numbers $\{\sigma_{kk}\}_{k=1}^{K}$ are the positive square roots of the eigenvalues of $\boldsymbol{R} \triangleq \boldsymbol{S}^T\boldsymbol{S}$, and hence are uniquely determined. The columns of the $N \times N$ matrix $\boldsymbol{W}$ are the orthonormal eigenvectors of $\boldsymbol{S}\boldsymbol{S}^T$, and the columns of the $K \times K$ matrix $\boldsymbol{V}$ are the orthonormal eigenvectors of $\boldsymbol{R} = \boldsymbol{S}^T\boldsymbol{S}$. We have the following result.

*Lemma 3:* The $N \times N$ diagonal matrix $\mathbf{\Lambda}_0^\dagger$ is given by

$$\mathbf{\Lambda}_0^\dagger = \boldsymbol{U}^T\boldsymbol{W}\mathbf{\Sigma}^{\dagger T}\boldsymbol{V}^T\boldsymbol{A}^{-1}\boldsymbol{V}\mathbf{\Sigma}^\dagger\boldsymbol{W}^T\boldsymbol{U} \tag{26}$$

where the $\mathbf{\Sigma}^\dagger$ is the transpose of $\mathbf{\Sigma}$ in which the positive singular values of $\boldsymbol{S}$ are replaced by their reciprocals.

*Proof:* See Appendix I. □

Using the above result, the following properties regarding the decorrelating detector $\boldsymbol{d}_1$ given by (13) can be verified.

*Lemma 3:* The decorrelating detector $\boldsymbol{d}_1$ given by (13) satisfies the following:

$$\boldsymbol{d}_1^T\boldsymbol{s}_1 = 1 \tag{27}$$
$$\boldsymbol{d}_1^T\boldsymbol{s}_k = 0, \qquad \text{for } k = 2, \cdots, K \tag{28}$$
$$\boldsymbol{d}_1^T\boldsymbol{d}_1 = [\boldsymbol{R}^{-1}]_{11}. \tag{29}$$

*Proof:* See Appendix II. □

Now it follows from Lemma 4 that the near–far resistance of the decorrelating detector $\boldsymbol{d}_1$ in (13) and that of the linear MMSE detector $\boldsymbol{m}_1$ in (18) is given by $\overline{\eta}_1 = 1/[\boldsymbol{R}^{-1}]_{11}$. To see this, first note that since as $\sigma \to 0$, the two linear detectors become identical, they have the same asymptotic multiuser efficiency (MAE) and near–far resistance. Hence it suffices to find the near–far resistance of the decorrelating detector $\boldsymbol{d}_1$ in (13). By Lemma 4 the output of $\boldsymbol{d}_1$ contains only the useful signal and the ambient Gaussian noise. The amplitude of the useful signal at the output is $A_1(\boldsymbol{d}_1^T\boldsymbol{s}_1) = A_1$; the variance of the noise is $\sigma^2(\boldsymbol{d}_1^T\boldsymbol{d}_1) = \sigma^2[\boldsymbol{R}^{-1}]_{11}$. The probability of error is then given by

$$P_1(\sigma) = Q\left(\frac{A_1\boldsymbol{d}_1^T\boldsymbol{s}_1}{\sigma\sqrt{\boldsymbol{d}_1^T\boldsymbol{d}_1}}\right) = Q\left(\frac{A_1}{\sigma\sqrt{[\boldsymbol{R}^{-1}]_{11}}}\right).$$

Therefore, $\eta_1 = \overline{\eta}_1 = 1/[\boldsymbol{R}^{-1}]_{11}$.

### *E. Asymptotics of Detector Estimates*

So far we have assumed that the exact signal autocorrelation matrix $\boldsymbol{C}$, and therefore its eigencomponents, are known. In practice, the eigencompoments of the sample autocorrelation matrix based on $n$ received data vectors

$$\hat{\boldsymbol{C}}(n) \triangleq \frac{1}{n}\sum_{i=1}^{n} \boldsymbol{r}(i)\boldsymbol{r}(i)^T \tag{30}$$

are used for constructing the subspace-based linear detectors (13) and (18). In this section, we examine the consistency and asymptotic variance of the estimates of the two linear detectors. Since the decision rule (9) is invariant to positive scaling on the linear detectors, for simplicity we consider the scaled version of the linear detectors $\boldsymbol{m}_1$ and $\boldsymbol{d}_1$, given, respectively, by

$$\boldsymbol{m} \triangleq \boldsymbol{U}_s\mathbf{\Lambda}_s^{-1}\boldsymbol{U}_s^T\boldsymbol{s}_1 \tag{31}$$
$$\boldsymbol{d} \triangleq \boldsymbol{U}_s(\mathbf{\Lambda}_s - \sigma^2\boldsymbol{I}_K)^{-1}\boldsymbol{U}_s^T\boldsymbol{s}_1 \tag{32}$$

and their respective estimated versions, given by

$$\hat{\boldsymbol{m}}(n) \triangleq \hat{\boldsymbol{U}}_s(n)\hat{\mathbf{\Lambda}}_s(n)^{-1}\hat{\boldsymbol{U}}_s(n)^T\boldsymbol{s}_1 \tag{33}$$
$$\hat{\boldsymbol{d}}(n) \triangleq \hat{\boldsymbol{U}}_s(n)[\hat{\mathbf{\Lambda}}_s(n) - \hat{\sigma}(n)^2\boldsymbol{I}_K]^{-1}\hat{\boldsymbol{U}}_s(n)^T\boldsymbol{s}_1 \tag{34}$$

where $\hat{\boldsymbol{U}}_s(n)$, $\hat{\mathbf{\Lambda}}_s(n)$, and $\hat{\sigma}(n)$ are the eigencomponents of $\hat{\boldsymbol{C}}(n)$, i.e.,

$$\hat{\boldsymbol{C}}(n) = \hat{\boldsymbol{U}}_s(n)\hat{\mathbf{\Lambda}}_s(n)\hat{\boldsymbol{U}}_s(n)^T + \hat{\sigma}(n)^2\hat{\boldsymbol{U}}_n(n)\hat{\boldsymbol{U}}_n(n)^T. \tag{35}$$

Assume that the received signal samples are independent and identically distributed (i.i.d.). Then the sample mean $\hat{\boldsymbol{C}}(n)$ converges to $\boldsymbol{C}$ almost surely (a.s.). It then follows [36] that as $n \to \infty$, $\hat{\lambda}_k(n) \to \lambda_k$ a.s., and $\hat{\boldsymbol{u}}_k(n) \to \boldsymbol{u}_k$ a.s., for $k = 1, \cdots, K$. Therefore, we have

$$\hat{\boldsymbol{m}}(n) = \sum_{k=1}^{K} \frac{1}{\hat{\lambda}_k}\hat{\boldsymbol{u}}_k(n)\hat{\boldsymbol{u}}_k(n)^T\boldsymbol{s}_1 \to \sum_{k=1}^{K}\frac{1}{\lambda_k}\boldsymbol{u}_k\boldsymbol{u}_k^T\boldsymbol{s}_1 = \boldsymbol{m} \ \text{a.s.} \quad \text{as } n \to \infty. \tag{36}$$

Similarly, $\hat{\boldsymbol{d}}(n) \to \boldsymbol{d}$ a.s. as $n \to \infty$. Hence both the estimated linear multiuser detectors (33) and (34) based on the received signal are *strongly consistent*. However, it is in general biased for finite number of samples. We next consider the asymptotic bound on the estimation errors.

First, for all eigenvalues and the $K$ largest eigenvectors of $\hat{\boldsymbol{C}}(n)$, the following bounds hold a.s. [36], [43]:

$$|\hat{\lambda}_k(n) - \lambda_k| = O(\sqrt{\log\log n/n}), \qquad \text{for } k = 1, \cdots, N$$
$$\|\hat{\boldsymbol{u}}_k(n) - \boldsymbol{u}_k\| = O(\sqrt{\log\log n/n}), \qquad \text{for } k = 1, \cdots, K.$$

Using these bounds, we have

$$\begin{aligned}
\|\boldsymbol{m} - \hat{\boldsymbol{m}}\| &= \|(\boldsymbol{U}_s\mathbf{\Lambda}_s^{-1}\boldsymbol{U}_s^T - \hat{\boldsymbol{U}}_s\hat{\mathbf{\Lambda}}_s^{-1}\hat{\boldsymbol{U}}_s^T)\boldsymbol{s}_1\| \\
&\leq \|(\boldsymbol{U}_s\mathbf{\Lambda}_s^{-1}\boldsymbol{U}_s^T - \hat{\boldsymbol{U}}_s\hat{\mathbf{\Lambda}}_s^{-1}\hat{\boldsymbol{U}}_s^T)\| \, \|\boldsymbol{s}_1\| \\
&= \|(\boldsymbol{U}_s\mathbf{\Lambda}_s^{-1}\boldsymbol{U}_s^T - \hat{\boldsymbol{U}}_s\mathbf{\Lambda}_s^{-1}\boldsymbol{U}_s^T) \\
&\quad + (\hat{\boldsymbol{U}}_s\mathbf{\Lambda}_s^{-1}\boldsymbol{U}_s^T - \hat{\boldsymbol{U}}_s\mathbf{\Lambda}_s^{-1}\hat{\boldsymbol{U}}_s^T) \\
&\quad + \hat{\boldsymbol{U}}_s(\mathbf{\Lambda}_s^{-1} - \hat{\mathbf{\Lambda}}_s^{-1})\hat{\boldsymbol{U}}_s^T\| \\
&\leq \|\boldsymbol{U}_s - \hat{\boldsymbol{U}}_s\| \, \|\mathbf{\Lambda}_s^{-1}\boldsymbol{U}_s^T\| \\
&\quad + \|\hat{\boldsymbol{U}}_s\mathbf{\Lambda}_s^{-1}\| \, \|\boldsymbol{U}_s - \hat{\boldsymbol{U}}_s\| \\
&\quad + \|\hat{\boldsymbol{U}}_s\| \, \|\mathbf{\Lambda}_s^{-1} - \hat{\mathbf{\Lambda}}_s^{-1}\| \, \|\hat{\boldsymbol{U}}_s\|.
\end{aligned} \tag{37}$$

Note that $\|\mathbf{\Lambda}_s^{-1}\boldsymbol{U}_s^T\|$, $\|\hat{\boldsymbol{U}}_s\mathbf{\Lambda}_s^{-1}\|$, and $\|\hat{\boldsymbol{U}}_s\|$ are all bounded. On the other hand, it is easily seen that

$$\|\boldsymbol{U}_s - \hat{\boldsymbol{U}}_s\| = \sum_{k=1}^{K}\|\boldsymbol{u}_k - \hat{\boldsymbol{u}}_k\| = O(\sqrt{\log\log n/n}) \ \text{a.s.}$$

and

$$\begin{aligned}
\|\mathbf{\Lambda}_s^{-1} - \hat{\mathbf{\Lambda}}_s^{-1}\| &= \sum_{k=1}^{K}|\lambda_k - \hat{\lambda}_k|/(\lambda_k\hat{\lambda}_k) \\
&= O(\sqrt{\log\log n/n}) \ \text{a.s.}
\end{aligned}$$

Therefore, we obtain the asymptotic estimation error for the linear MMSE detector, and similarly that for the decorrelating detector, given, respectively, by

$$\|\hat{\boldsymbol{m}}(n) - \boldsymbol{m}\| = O(\sqrt{\log\log n/n}) \quad \text{a.s.} \tag{38}$$

$$\|\hat{\boldsymbol{d}}(n) - \boldsymbol{d}\| = O(\sqrt{\log\log n/n}) \quad \text{a.s.} \tag{39}$$

## IV. Blind Adaptive Multiuser Detection Based on Subspace Tracking

### A. Tracking the Signal Subspace

It is seen from the previous section that the linear multiuser detectors are obtained as long as the signal subspace components are identified. The classic approach to subspace estimation is through batch eigenvalue decomposition (ED) of the sample autocorrelation matrix, or batch singular value decomposition (SVD) of the data matrix, which is computationally too expensive for adaptive applications. Modern subspace tracking algorithms are recursive in nature and update the subspace in a sample-by-sample fashion. Various subspace tracking algorithms exist in the literature, e.g., [3], [5], [6], [29], [33], and [41]. In this paper, we adopt the recently proposed projection approximation subspace tracking (PASTd) algorithm [41] for the blind adaptive multiuser detection application. The advantages of this algorithm include almost sure global convergence to the signal eigenvectors and eigenvalues, low computational complexity $(O(NK))$, and the rank tracking capability. We next briefly review the PASTd algorithm for tracking the signal subspace.

Let $\boldsymbol{r} \in \mathcal{R}^N$ be a random vector with autocorrelation matrix $\boldsymbol{C} = E\{\boldsymbol{r}\, \boldsymbol{r}^T\}$. Consider the scalar function

$$\begin{aligned} J(\boldsymbol{W}) &= E\{\|\boldsymbol{r} - \boldsymbol{W}\boldsymbol{W}^T\boldsymbol{r}\|^2\} \\ &= \operatorname{tr}(\boldsymbol{C}) - 2\operatorname{tr}(\boldsymbol{W}^T\boldsymbol{C}\boldsymbol{W}) + \operatorname{tr}(\boldsymbol{W}^T\boldsymbol{C}\boldsymbol{W}\boldsymbol{W}^T\boldsymbol{W}) \end{aligned} \tag{40}$$

with a matrix argument $\boldsymbol{W} \in \mathcal{R}^{N\times r}$ $(r < N)$. It is shown in [41] that

- $\boldsymbol{W}$ is a stationary point of $J(\boldsymbol{W})$ if and only if $\boldsymbol{W} = \boldsymbol{U}_r\boldsymbol{Q}$, where $\boldsymbol{U}_r \in \mathcal{R}^{N\times r}$ contains any $r$ distinct eigenvectors of $\boldsymbol{C}$ and $\boldsymbol{Q} \in \mathcal{R}^{r\times r}$ is any unitary matrix.
- All stationary points of $J(\boldsymbol{W})$ are saddle points except when $\boldsymbol{U}_r$ contains the $r$ dominant eigenvectors of $\boldsymbol{C}$. In that case, $J(\boldsymbol{W})$ attains the global minimum.

Therefore, for $r = 1$, the solution of minimizing $J(\boldsymbol{W})$ is given by the most dominant eigenvector of $\boldsymbol{C}$. In applications, only sample vectors $\boldsymbol{r}(i)$ are available. Replacing (40) with the exponentially weighted sums yields

$$J[\boldsymbol{W}(t)] = \sum_{i=1}^{t} \beta^{t-i}\|\boldsymbol{r}(i) - \boldsymbol{W}(t)\boldsymbol{W}(t)^T\boldsymbol{r}(i)\|^2. \tag{41}$$

The key issue of the PASTd approach is to approximate $\boldsymbol{W}(t)^T\boldsymbol{r}(i)$ in (41), the unknown projection of $\boldsymbol{r}(i)$ onto the columns of $\boldsymbol{W}(t)$, by $\boldsymbol{y}(i) = \boldsymbol{W}(i-1)^T\boldsymbol{r}(i)$, which can be calculated for $1 \le i \le t$ at time $t$. This results in a modified cost function

$$\tilde{J}[\boldsymbol{W}(t)] = \sum_{i=1}^{t} \beta^{t-i}\|\boldsymbol{r}(i) - \boldsymbol{W}(t)\boldsymbol{y}(i)\|^2. \tag{42}$$

The recursive least squares (RLS) algorithm can then be used to solve for $\boldsymbol{W}(t)$ that minimizes the exponentially weighted least squares criterion (42).

The PASTd algorithm for tracking the eigenvalues and eigenvectors of the signal subspace is based on the deflation technique and its basic idea is as follows. For $r = 1$ by minimizing $\tilde{J}(\boldsymbol{W}(t))$ in (42) the most dominant eigenvector is updated. Then the projection of the current data vector $\boldsymbol{r}(t)$ onto this eigenvector is removed from $\boldsymbol{r}(t)$ itself. Now the second most dominant eigenvector becomes the most dominant one in the updated data vector and it can be extracted similarly. We apply this procedure repeatedly until all the $K$ eigenvectors are estimated sequentially.

Based on the estimated eigenvalues, using information-theoretic criteria such as the Akaike information criterion (AIC) or minimum description length (MDL) criterion [39], the rank of the signal subspace, or equivalently, the number of active users in the channel, can be estimated adaptively as well [40]. The quantities AIC and MDL are defined as follows:

$$\text{AIC}\,(k) \triangleq (N-k)L\ln\alpha(k) + k(2N-k) \tag{43}$$

$$\text{MDL}\,(k) \triangleq (N-k)L\ln\alpha(k) + \frac{k}{2}\,(2N-k)\ln L \tag{44}$$

where $L$ is the number of data samples used in the estimation. When an exponentially weighted window with forgetting factor $\beta$ is applied to the data, the equivalent number of data samples is $L = 1/(1-\beta)$. $\alpha(k)$ in the above definitions is defined as

$$\alpha(k) = \frac{\left(\sum_{i=k+1}^{N}\hat{\lambda}_i\right)\Big/(N-k)}{\left(\prod_{i=k+1}^{N}\hat{\lambda}_i\right)^{1/(N-k)}}. \tag{45}$$

The estimate of rank is given by the value $k$ that minimizes the the quantity (43) or (44). Finally, the algorithm for both rank and signal subspace tracking is summarized in Table I. The computational complexity of this algorithm is $(4K+3)N + O(K) = O(NK)$. The convergence dynamics of the PASTd algorithm are studied in [42]. It is shown there that with the forgetting factor $\beta = 1$ under mild conditions, this algorithm globally converges almost surely to the signal eigenvectors and eigenvalues.

### B. Simulation Examples

In this section we provide two simulation examples to illustrate the performance of the subspace-based blind adaptive linear MMSE detector.

*Example 1:* This example compares the performance of the subspace-based blind MMSE detector with the performance

TABLE I
THE PASTd (PROJECTION APPROXIMATION SUBSPACE TRACKING WITH DEFLATION) ALGORITHM [40], [41] FOR TRACKING BOTH THE RANK AND SIGNAL SUBSPACE COMPONENTS OF THE RECEIVED SIGNAL $r(t)$. THE RANK ESTIMATION IS BASED ON THE AKAIKE INFORMATION CRITERION (AIC)

| Updating the eigenvalues and eigenvectors of signal subspace $\{\lambda_k,\ \mathbf{u}_k\}_{k=1}^{K}$ | | | |
|---|---|---|---|
| | $\mathbf{x}_1(t)$ | $=$ | $\mathbf{r}(t)$ |
| FOR | $k = 1{:}K_{t-1}$ | DO | |
| | $y_k(t)$ | $=$ | $\mathbf{u}_k^H(t-1)\mathbf{x}_k(t)$ |
| | $\lambda_k(t)$ | $=$ | $\beta\lambda_k(t-1) + \lvert y_k(t)\rvert^2$ |
| | $\mathbf{u}_k(t)$ | $=$ | $\mathbf{u}_k(t-1) + [\mathbf{x}_k(t) - \mathbf{u}_k(t-1)y_k(t)]\, y_k(t)^*/\lambda_k(t)$ |
| | $\mathbf{x}_{k+1}(t)$ | $=$ | $\mathbf{x}_k(t) - \mathbf{u}_k(t)y_k(t)$ |
| END | | | |
| | $\sigma^2(t)$ | $=$ | $\beta\sigma^2(t-1) + \lVert\mathbf{x}_{K_{t-1}+1}(t)\rVert^2/(N - K_{t-1})$ |
| Updating the rank of signal subspace $K_t$ | | | |
| FOR | $k = 1{:}K_{t-1}$ | DO | |
| | $\alpha(k)$ | $=$ | $\left[\sum_{i=k+1}^{N} \lambda_i(t)/N - k\right] / \left(\prod_{i=k+1}^{N} \lambda_i(t)\right)^{\frac{1}{N-k}}$ |
| | $\mathrm{AIC}(k)$ | $=$ | $(N-k)\ln[\alpha(k)]/(1-\beta) + k(2N-k)$ |
| END | | | |
| | $K_t$ | $=$ | $\arg\min_{0\le k\le N-1} \mathrm{AIC}(k) + 1$ |
| IF | $K_t < K_{t-1}$ | THEN | |
| | remove $\{\lambda_k(t), \mathbf{u}_k(t)\}_{k=K_t+1}^{K_{t-1}}$ | | |
| ELSE IF | $K_t > K_{t-1}$ | THEN | |
| | $\mathbf{u}_{K_t}(t)$ | $=$ | $\mathbf{x}_{K_{t-1}+1}(t)/\lVert\mathbf{x}_{K_{t-1}+1}(t)\rVert$ |
| | $\lambda_{K_t}(t)$ | $=$ | $\sigma^2(t)$ |
| END | | | |

of the minimum-output-energy (MOE) blind adaptive detector proposed in [7]. It assumes a synchronous CDMA system with processing gain $N = 31$ and six users $(K = 6)$. The desired user is user 1. There are four 10-dB multiple-access interferers (MAI's) and one 20-dB MAI, i.e., $A_k^2/A_1^2 = 10$, for $k = 2, \cdots, 5$, and $A_k^2/A_1^2 = 100$, for $k = 6$. The performance measure is the output signal-to-interference ratio (SIR), defined as $\mathrm{SIR} \triangleq E^2\{\boldsymbol{m}^T\boldsymbol{r}\}/\mathrm{Var}\{\boldsymbol{m}^T\boldsymbol{r}\}$, where the expectation is with respect to the data bits of MAI's and the noise. In the simulation, the expectation operation is replaced by the time averaging operation. For the PASTd subspace tracking algorithm, we found that with a random initialization, the convergence is fairly slow. Therefore, in the simulations, the initial estimates of the eigencomponents of the signal subspace are obtained by applying an SVD to the first 50 data vectors. The PASTd algorithm is then employed for tracking the signal subspace. The time averaged output SIR versus number of iterations is plotted in Fig. 1.

As a comparison, the simulated performance of the recursive least squared (RLS) version of the MOE blind adaptive detector is also shown in Fig. 1. It has been shown in [26] that the steady-state SIR of this algorithm is given by $\mathrm{SIR}^\infty = \mathrm{SIR}^*/(1 + d + d \cdot \mathrm{SIR}^*)$, where $\mathrm{SIR}^*$ is the optimal SIR value, and $d \triangleq (1 - \beta/2\beta)N$ $(0 < \beta < 1$ is the forgetting factor). Hence the performance of this algorithm is upper-bounded by $1/d$ when $1/d \ll \mathrm{SIR}^*$, as is seen in Fig. 1. Although an analytical expression for the steady-state SIR of the subspace-based blind adaptive detector is very difficult to obtain, as the dynamics of the PASTd algorithm are fairly complicated, it is seen from Fig. 1 that with the same forgetting factor $\beta$, this new blind adaptive detector well outperforms the RLS MOE detector. Moreover, the RLS MOE detector has a computational complexity of $O(N^2)$ per iteration, whereas the complexity per iteration of the proposed detector is $O(NK)$.

*Example 2:* This example illustrates the performance of the proposed blind adaptive detector in a dynamic multiple-access channel where interferers may enter or exit the channel. The simulation starts with six 10-dB MAI's in the channel; at $t = 2000$, a 20-dB MAI enters the channel; at $t = 4000$, the 20-dB MAI and three of the 10-dB MAI's exit the channel. The performance of the proposed detector is plotted in Fig. 2. It is seen that this subspace-based blind adaptive multiuser detector can adapt rapidly to the dynamic channel traffic.

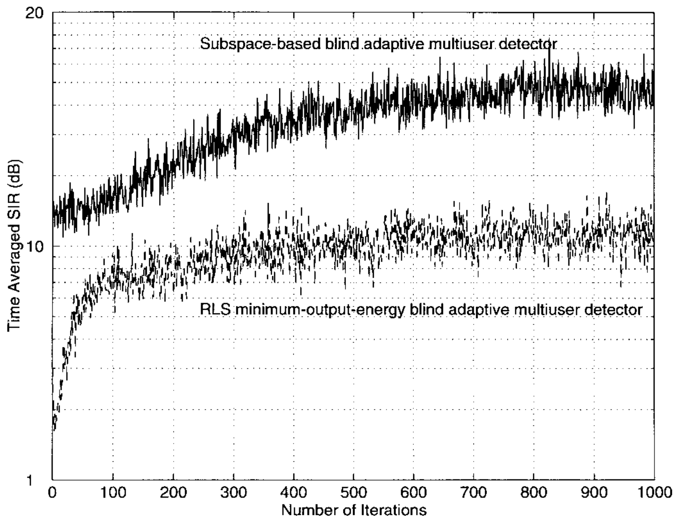


Fig. 1. Performance comparison between the subspace-based blind linear MMSE multiuser detector and the RLS MOE blind adaptive detector. The processing gain $N = 31$. There are four 10-dB MAI's and one 20-dB MAI in the channel, all relative to the desired user's signal. The signature sequence of the desired user is an $m$-sequence, while the signature sequences of the MAI's are randomly generated. The signal-to-ambient-noise ratio after despreading is 20 dB. The forgetting factor used in both algorithms is $\beta = 0.995$. The data plotted are the average over 100 simulations.

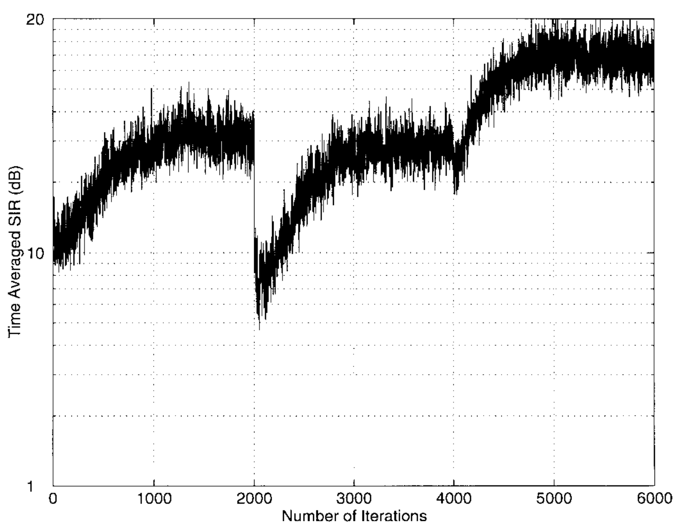


Fig. 2. Performance of the subspace-based blind linear MMSE multiuser detector in a dynamic multiple-access channel where interferers may enter or exit the channel. At $t = 0$, there are six 10-dB MAI's in the channel; at $t = 2000$, a 20-dB MAI enters the channel; at $t = 4000$, the 20-dB MAI and three of the 10-dB MAI's exit the channel. The processing gain $N = 31$. The signal-to-noise ratio after despreading is 20 dB. The forgetting factor is $\beta = 0.995$. The data plotted are the average over 100 simulations.

## V. Mismatch and Blind Adaptive Multipath Channel Estimation

### A. Asymptotic Multiuser Efficiency Under Mismatch

We now consider the effect of signature waveform mismatch on the performance of the subspace-based linear multiuser detectors. Let $\tilde{\boldsymbol{s}}_1$ with $\|\tilde{\boldsymbol{s}}_1\| = 1$ be the assumed signature waveform of the user of interest, and $\boldsymbol{s}_1$ be the true signature waveform. $\tilde{\boldsymbol{s}}_1$ can then be decomposed into components of the signal subspace and noise subspace, i.e., $\tilde{\boldsymbol{s}}_1 = \tilde{\boldsymbol{s}}_1^s + \tilde{\boldsymbol{s}}_1^n$, where $\tilde{\boldsymbol{s}}_1^s \in \text{range}\,(\boldsymbol{U}_s)$ and $\tilde{\boldsymbol{s}}_1^n \in \text{range}\,(\boldsymbol{U}_n)$. The signal subspace component $\tilde{\boldsymbol{s}}_1^s$ can then be written as

$$\tilde{\boldsymbol{s}}_1^s = \alpha_1 \boldsymbol{s}_1 + \alpha_2 \boldsymbol{s}_2 + \cdots + \alpha_K \boldsymbol{s}_K = \boldsymbol{S}\underline{\alpha}$$

for some $\underline{\alpha} \in \mathcal{R}^K$.

*Proposition 3:* The asymptotic multiuser efficiency of the decorrelating detector $\boldsymbol{d}_1$ in (13) and that of the linear MMSE detector $\boldsymbol{m}_1$ in (18) under the signature waveform mismatch is given by

$$\eta_1 = \frac{\max^2\left\{0, |\alpha_1| - \sum_{k=2}^{K} |\alpha_k| \,\dfrac{A_1}{A_k}\right\}}{A_1^4 \underline{\alpha}^T \boldsymbol{A}^{-1}\boldsymbol{R}^{-1}\boldsymbol{A}^{-1}\underline{\alpha}}. \tag{46}$$

*Proof:* Since $\boldsymbol{d}_1$ and $\boldsymbol{m}_1$ have the same asymptotic multiuser efficiency (AME), we only need to compute the AME for $\boldsymbol{d}_1$. Because a positive scaling on the detector does not affect its AME, we consider the AME of the following scaled version of $\boldsymbol{d}_1$ under the signature waveform mismatch:

$$\begin{aligned}\tilde{\boldsymbol{d}} &\triangleq \boldsymbol{U}_s(\boldsymbol{\Lambda}_s - \sigma^2 \boldsymbol{I}_K)^{-1}\boldsymbol{U}_s^T \tilde{\boldsymbol{s}}_1\\ &= \boldsymbol{U}_s(\boldsymbol{\Lambda}_s - \sigma^2 \boldsymbol{I}_K)^{-1}\boldsymbol{U}_s^T \boldsymbol{S}\underline{\alpha}\\ &= \boldsymbol{U}\boldsymbol{\Lambda}_0^{\dagger}\boldsymbol{U}^T\boldsymbol{S}\underline{\alpha}\end{aligned} \tag{47}$$

where the second equality follows from the fact that the noise subspace component $\tilde{\boldsymbol{s}}_1^n$ is orthogonal to the signal subspace $\boldsymbol{U}_s$; and the third equality follows from (8). Now following the same lines of derivation as in (67) and in (69), we obtain

$$\tilde{\boldsymbol{d}}^T\boldsymbol{s}_k = \underline{\alpha}^T\boldsymbol{A}^{-1}\boldsymbol{e}_k = A_k^{-2}\alpha_k \tag{48}$$

$$\tilde{\boldsymbol{d}}^T\tilde{\boldsymbol{d}} = \underline{\alpha}^T\boldsymbol{A}^{-1}\boldsymbol{R}^{-1}\boldsymbol{A}^{-1}\underline{\alpha}. \tag{49}$$

Using (5) and (48), the output of $\tilde{\boldsymbol{d}}$ is then

$$\begin{aligned}\tilde{\boldsymbol{d}}^T\boldsymbol{r} &= \tilde{\boldsymbol{d}}^T\left(\sum_{k=1}^{K} A_k b_k \boldsymbol{s}_k + \sigma\boldsymbol{n}\right)\\ &= \sum_{k=1}^{K} A_k^{-1}\alpha_k b_k + \sigma\tilde{\boldsymbol{d}}^T\boldsymbol{n}\end{aligned} \tag{50}$$

where $\text{Var}\,(\tilde{\boldsymbol{d}}^T\boldsymbol{n}) = \tilde{\boldsymbol{d}}^T\tilde{\boldsymbol{d}}$. The probability of error for user 1 is then given by

$$\begin{aligned}P_1(\sigma) = \frac{1}{2^{K-1}} &\sum_{(b_2,\cdots,b_K)\in\{-1,1\}^{K-1}}\\ &\cdot Q\left(\frac{A_1}{\sigma}\cdot\frac{\alpha_1 - \sum_{k=2}^{K}\alpha_k b_k \dfrac{A_1}{A_k}}{\sqrt{A_1^4\underline{\alpha}^T\boldsymbol{A}^{-1}\boldsymbol{R}^{-1}\boldsymbol{A}^{-1}\underline{\alpha}}}\right).\end{aligned} \tag{51}$$

It then follows that the asymptotic multiuser efficiency is given by (46). □

*Remark 3:* It is seen from (51) that signature waveform mismatch causes MAI leakage at the detector output. Strong interferers $(A_k \gg A_1)$ are suppressed at the output, whereas weak interferers $(A_k \ll A_1)$ may lead to performance degradation. If the mismatch is not significant, with power control, so that the open eye condition is satisfied (i.e., $|\alpha_1| > \Sigma_{k=2}^{K} |\alpha_k| \frac{A_1}{A_k}$), then the performance loss is negligible; otherwise, the effective signature waveform should be estimated first, as will be discussed in the following section. Moreover, since the mismatched signature waveform $\tilde{\boldsymbol{s}}_1$ is first projected onto the signal subspace, its noise subspace component $\tilde{\boldsymbol{s}}_1^n$ is nulled out and does not cause performance degradation; whereas for the blind adaptive MOE detector, such a noise subspace component may lead to complete cancellation of both the signal and MAI without energy constraint on the detector [7]. We note that adaptive MOE filtering in the signal subspace has been proposed recently in [9] and [10]. The result in this paper indicates, however, that adaptive filtering in the signal subspace is not needed if the signal subspace parameters $(\boldsymbol{U}_s, \boldsymbol{\Lambda}_s, \sigma)$ are identified, because the linear multiuser detectors can be expressed in closed form by these parameters.

### *B. Blind Adaptive Estimation of Multipath Channel Response*

When the signal is transmitted over a multipath channel, at the receiver end, the effective signature waveform is the multipath channel response to the original signature waveform. Subspace-based batch methods have been proposed for blind multipath channel estimation [2], [14]. In this section, we develop a blind adaptive method for channel estimation, which can be combined with the subspace tracking algorithm for joint channel estimation and multiuser detection.

Suppose that $K$ users are transmitting synchronously over a multipath channel. The number of resolvable paths for each user is $L = \lceil WT_m \rceil$ [27], where $W$ is the signal bandwidth and $T_m$ is the channel multipath spread. The impulse response of such a multipath channel for the $k$th user can be represented by a tapped delayed line

$$h_k(t) = \sum_{l=1}^{L} h_{k,l}\delta(t-(l-1)T_c) \tag{52}$$

where $T_c = 1/W$ is the chip period and the coefficients $h_{k,l}$ are complex channel gains. For the data signaling interval much longer than the multipath delay spread, i.e., $T \gg T_m \approx L/W$, any intersymbol interference (ISI) due to channel dispersion can be neglected [27]. Therefore, the complex $N$-vector of chip-matched filter output within a symbol interval is

$$\begin{aligned}\boldsymbol{r} &= \sum_{k=1}^{K} A_k b_k \sum_{l=1}^{L} h_{k,l}\boldsymbol{s}_{k,l} + \sigma\boldsymbol{n} \\ &= \sum_{k=1}^{K} A_k b_k \tilde{\boldsymbol{s}}_k + \sigma\boldsymbol{n}\end{aligned} \tag{53}$$

where $\boldsymbol{s}_{k,l}$ is the vector representation of the delayed user signature waveform $s_k(t-(l-1)T_c)$; $\boldsymbol{n}$ is a complex Gaussian noise vector with mean $\boldsymbol{0}$ and covariance matrix $\boldsymbol{I}$; $\tilde{\boldsymbol{s}}_k \triangleq \boldsymbol{S}_k\boldsymbol{h}_k$ is the received composite signature waveform of the $k$th user, where

$$\boldsymbol{S}_k \triangleq [\boldsymbol{s}_{k,1}\ \boldsymbol{s}_{k,2} \cdots \boldsymbol{s}_{k,L}]$$

and

$$\boldsymbol{h}_k \triangleq [h_{k,1}\ h_{k,2} \cdots h_{k,L}]^T.$$

Suppose that the signal subspace is identified as $\tilde{\boldsymbol{U}}_s = [\tilde{\boldsymbol{u}}_1\ \tilde{\boldsymbol{u}}_2 \cdots \tilde{\boldsymbol{u}}_K]$. Since $\tilde{\boldsymbol{s}}_1 \in \text{range}\ (\tilde{\boldsymbol{U}}_s)$, there exists $\boldsymbol{f}_1 \in \mathcal{C}^K$ such that $\tilde{\boldsymbol{s}}_1 = \tilde{\boldsymbol{U}}_s\boldsymbol{f}_1$. On the other hand, we also have $\tilde{\boldsymbol{s}}_1 = \boldsymbol{S}_1\boldsymbol{h}_1$. Therefore, $\tilde{\boldsymbol{s}}_1$ is given by one solution to the linear equation system $\boldsymbol{S}_1\boldsymbol{h}_1 = \tilde{\boldsymbol{U}}_s\boldsymbol{f}_1$. And obviously $\tilde{\boldsymbol{s}}_1$ is uniquely determined if and only if $\text{rank}\ [\text{range}\ (\boldsymbol{S}_1) \cap \text{range}\ (\tilde{\boldsymbol{U}}_s)] = 1$. In the following, we assume that this uniqueness condition is satisfied and develop a recursive method for estimating multipath channel response $\boldsymbol{h}_1$ based on $\boldsymbol{S}_1$ and $\tilde{\boldsymbol{U}}_s$.

Since in practice $\tilde{\boldsymbol{U}}_s$ is always a noisy estimate of the true signal subspace, we need to solve $\boldsymbol{S}_1\boldsymbol{h}_1 = \tilde{\boldsymbol{U}}_s\boldsymbol{f}_1$ in the least squares sense. Define $\boldsymbol{D} \triangleq [\tilde{\boldsymbol{U}}_s\ \boldsymbol{S}_1]$ and $\boldsymbol{x} \triangleq [\boldsymbol{f}_1^T\ -\boldsymbol{h}_1^T]^T$, then $\boldsymbol{h}_1$ is contained in the solution $\boldsymbol{x}$ to the following optimization problem

$$\min_{\boldsymbol{x}\in\mathcal{C}^{K+L}} \|\boldsymbol{D}\boldsymbol{x}\|^2 = \boldsymbol{x}^H\boldsymbol{D}^H\boldsymbol{D}\boldsymbol{x}, \quad \text{s.t.} \quad \|\boldsymbol{x}\|^2 = 1. \tag{54}$$

It is well known that the solution to (54) is given by the minimum eigenvector of the matrix $\boldsymbol{D}^H\boldsymbol{D}$. Using the penalty function method [15], the constrained optimization problem (54) can be transformed into an unconstrained optimization problem by defining the function

$$q(\boldsymbol{x}, c) \triangleq \frac{1}{2}\boldsymbol{x}^H\boldsymbol{D}^H\boldsymbol{D}\boldsymbol{x} + \frac{c}{4}(\boldsymbol{x}^H\boldsymbol{x} - 1)^2 \tag{55}$$

where $c$ is some positive constant. The key to developing a recursive procedure for solving (54) is the following result, whose real number version is found in [19].

*Proposition 4:* $\boldsymbol{x}$ is a stationary point of $q(\boldsymbol{x}, c)$ if and only if $\boldsymbol{x}$ is a scaled version of an eigenvector of the matrix $\boldsymbol{D}^H\boldsymbol{D}$, with norm

$$\|\boldsymbol{x}\| = \sqrt{1 - \frac{\nu}{c}}$$

($\nu$ is the corresponding eigenvalue). Moreover, all stationary points of $q(\boldsymbol{x}, c)$ are saddle points except when $\boldsymbol{x}$ is a scaled version of the minimum eigenvector of $\boldsymbol{D}^H\boldsymbol{D}$. In that case, $q(\boldsymbol{x}, c)$ attains the global minimum.

*Proof:* See Appendix III. □

By the above result, any algorithm of gradient descent type for minimizing $q(\boldsymbol{x}, c)$ in (55) is guaranteed to converge to the minimum eigenvector of $\boldsymbol{B}$. The constant $c$ is required to be greater than the minimum eigenvalue of $\boldsymbol{B}$, which is close to 0. Choosing a large $c$ will force the norm of the solution $\boldsymbol{x}$ be close to 1.

Based on the above discussion, an adaptive algorithm for joint channel estimation and multiuser detection is readily obtained as follows. At time $t$, suppose that the signal subspace obtained by the subspace tracking algorithm is $\tilde{\boldsymbol{U}}_s(t)$. We form the matrix $\boldsymbol{D}(t) = [\tilde{\boldsymbol{U}}_s(t)\ \boldsymbol{S}_1]$ and compute the matrix

$\boldsymbol{B}(t) = \boldsymbol{D}(t)^H \boldsymbol{D}(t)$. We then apply one step of update on the estimated minimum eigenvector $\boldsymbol{x}(t)$ of $\boldsymbol{B}(t)$, according to the method of steepest descent

$$\boldsymbol{x}(t) = \boldsymbol{x}(t-1) - \mu[\boldsymbol{B}(t)\boldsymbol{x}(t-1) + c(\|\boldsymbol{x}(t-1)\|^2 - 1)\boldsymbol{x}(t-1)]. \quad (56)$$

The estimated channel gain vector $\boldsymbol{h}_1(t)$ is a subvector of $\boldsymbol{x}(t)$. Upon normalization, the effective signature waveform $\tilde{\boldsymbol{s}}_1(t)$ is found, which together with the estimated signal subspace components $\tilde{\boldsymbol{U}}_s(t)$ and $\tilde{\boldsymbol{\Lambda}}_s(t)$, is used to form the estimated linear MMSE detector $\boldsymbol{m}_1(t)$. The adaptive channel estimator proposed here differs from previous nonadaptive ones in that it performs on-line channel estimation. Moreover, this channel estimator is integrated with the linear multiuser detector and incurs little attendant computational overhead, compared with the computationally expensive SVD-based batch methods for channel estimation [2], [14]. Note that the estimated channel gain vector $\boldsymbol{h}_1(t)$, and therefore the estimated signature waveform $\tilde{\boldsymbol{s}}_1(t)$, has an arbitrary phase ambiguity, which can be easily resolved by differentially encoding the transmitted data.

*Example 3:* This example is to demonstrate the performance of the proposed blind adaptive algorithm for joint multipath channel estimation and multiuser detection. The number of resolvable paths $L = 3$. There are four 10-dB MAI's and one 20-dB MAI in the channel, as in Example 1. Fig. 3 shows the convergence behavior of the blind adaptive channel estimator. Fig. 4 shows the time-averaged SIR versus the number of iterations. It is seen that by employing the proposed algorithm, little performance degradation is incurred when the signal is distorted by the multipath channel.

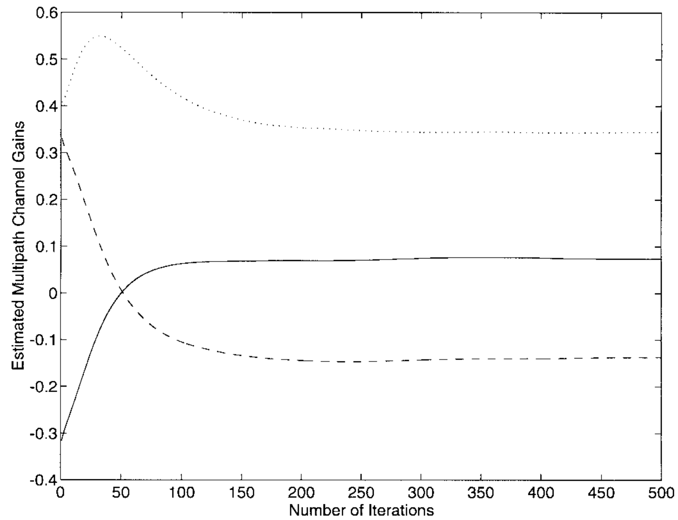


(a)

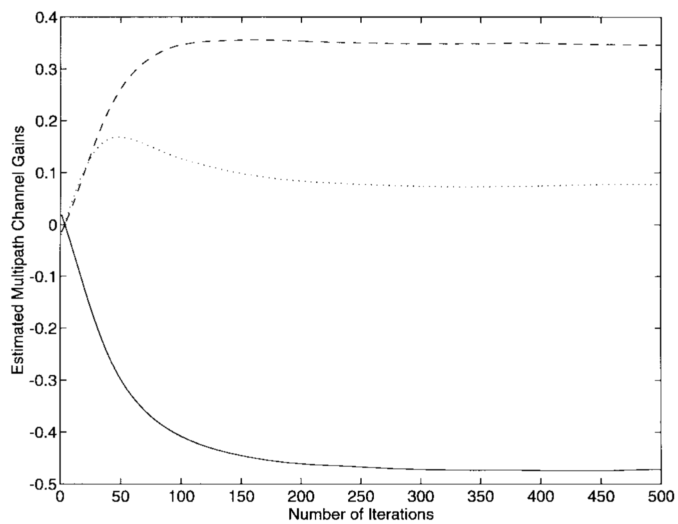


(b)

Fig. 3. Convergence of the blind adaptive multipath channel estimator. The number of resolvable paths $L = 3$. There are four 10-dB MAI's and one 20-dB MAI in the channel, relative to the desired user's signal. Shown in the figures are the real (a) and imaginary (b) components of the three estimated multipath gains versus the number of iterations.

## VI. Spatial Processing and Blind Adaptive Array Response Estimation

### A. Spatial Processing and Diversity Combining

One approach that shows promise for substantial capacity enhancement for CDMA systems is the use of spatial processing with multiple-sensor antenna arrays [23]. Combined multiuser detection and array processing has been considered previously, e.g., [12], [18], and [32]. However, one of the challenges in this area is to develop an efficient technique for estimating the array response to the desired user's signal. In this section, we consider a blind adaptive multiuser detector that employs spatial diversity in the form of an antenna array.

Suppose that an array of $J$ sensors is employed at the receiver. Let $\boldsymbol{a}_k$ be the $J$-vector of array response to the $k$th user. For a linear array, the $l$th component of this array response is given by

$$a_{kl} \triangleq [\boldsymbol{a}_k]_l = \exp(j\phi_{kl}) = \exp\left[j\frac{2\pi d}{\lambda}\left(l - \frac{J+1}{2}\right)\sin(\theta_k)\right] \quad (57)$$

where $d$ is the inter-sensor spacing, $\lambda$ is the wavelength of the carrier, and $\theta_k$ is the $k$th user signal's direction of arrival (DOA). The received signal at the $l$th sensor is then given by

$$\boldsymbol{r}_l = \sum_{k=1}^{K} A_k a_{kl} b_k \boldsymbol{s}_k + \sigma \boldsymbol{n}_l, \qquad l = 1, \cdots, J \quad (58)$$

where $\boldsymbol{n}_l$ is a complex Gaussian random vector with mean $\mathbf{0}$ and covariance matrix $\boldsymbol{I}_N$. Suppose that a bank of $J$ decorrelating detectors $\boldsymbol{d}_1^1, \cdots, \boldsymbol{d}_1^J$ are employed at the array output, one for each sensor. Let

$$\boldsymbol{z}_1 \triangleq [\boldsymbol{r}_1^T \boldsymbol{d}_1^1 \cdots \boldsymbol{r}_J^T \boldsymbol{d}_1^J]^T$$

be the output vector of the bank of decorrelators. Assuming that the noise $\{\boldsymbol{n}_l\}_{l=1}^J$ is spatially uncorrelated, then it is easily seen that the complex $J$-vector $\boldsymbol{z}_1$ has a Gaussian distribution, i.e., $\boldsymbol{z}_1 \sim \mathcal{N}_c(A_1 b_1 \boldsymbol{a}_1, [\boldsymbol{R}^{-1}]_{11}\sigma^2 \boldsymbol{I}_J)$. Therefore, the maximum-likelihood decision rule for $b_1$ based on $\boldsymbol{z}_1$ is

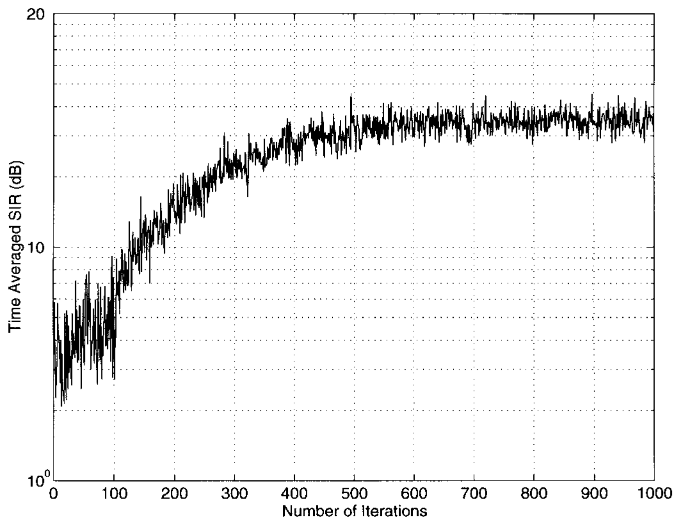


Fig. 4. Performance of the blind adaptive algorithm for joint effective signature waveform estimation and linear MMSE multiuser detection. The processing gain $N = 31$. There are four 10-dB MAI's and one 20-dB MAI in the channel. The signal-to-noise ratio after despreading is 20 dB. The number of resolvable paths $L = 3$. The data plotted are the average over 100 simulations.

given by [25]

$$\hat{b}_1 = \mathrm{sgn}\,[\mathrm{Re}\,(\boldsymbol{a}_1^H \boldsymbol{z}_1]. \tag{59}$$

If instead $\boldsymbol{z}_1$ is the output vector of the bank of linear MMSE detectors, its distribution is then approximately Gaussian [24] and hence the same decision rule can still be used. Therefore, the key issue here is to determine the array response vector $\boldsymbol{a}_1$. Once the array response (i.e., spatial signature) is accurately estimated, it is also possible to use joint space–time multiuser detection to achieve better performance.

### *B. Blind Adaptive Estimation of Array Response*

Since in general the number of users in the CDMA channels far exceeds the number of antennas, the conventional subspace techniques for DOA estimation such as MUSIC, ESPRIT, etc., are not applicable. However, based on the output vector $\boldsymbol{z}_1$ of the bank of linear multiuser detectors, a simple blind adaptive method for estimating the array response $\boldsymbol{a}_1$ can be developed as follows. Notice that the autocorrelation matrix of $\boldsymbol{z}_1$ is given by

$$\boldsymbol{Q}_1 \stackrel{\Delta}{=} E\{\boldsymbol{z}_1\, \boldsymbol{z}_1^H\} = A_1^2 \boldsymbol{a}_1 \boldsymbol{a}_1^H + [\boldsymbol{R}^{-1}]_{11} \sigma^2 \boldsymbol{I}_J. \tag{60}$$

It is seen from (60) that $\boldsymbol{a}_1$ is the principal eigenvector of $\boldsymbol{Q}_1$. Now as in the PASTd algorithm for subspace tracking, $\boldsymbol{a}_1$ is the unique global minimum point of the cost function

$$\mathcal{L}(\boldsymbol{a}) = E\{\|\boldsymbol{z}_1 - \boldsymbol{a}\boldsymbol{a}^H \boldsymbol{z}_1\|^2\}. \tag{61}$$

Consider the exponentially weighted version of the cost function (61)

$$\begin{aligned}\tilde{\mathcal{L}}[\boldsymbol{a}_1(t)] &= \sum_{i=1}^{t} \beta^{t-i} \|\boldsymbol{z}_1(i) - \boldsymbol{a}_1(t)\boldsymbol{a}_1(t)^H \boldsymbol{z}_1(i)\|^2 \\ &\approx \sum_{i=1}^{t} \beta^{t-i} \|\boldsymbol{z}_1(i) - \boldsymbol{a}_1(t) y(i)\|^2 \end{aligned} \tag{62}$$

TABLE II
BLIND ADAPTIVE ALGORITHM FOR ESTIMATING THE ANTENNA ARRAY RESPONSE $\boldsymbol{a}(t)$ TO THE DESIRED USER'S SIGNAL, BASED ON THE OUTPUT $\boldsymbol{z}(t)$ OF A BANK OF LINEAR MULTIUSER DETECTORS

| | | |
|---|---|---|
| $y(t)$ | $=$ | $\mathbf{a}^H(t-1)\mathbf{z}(t)$ |
| $\lambda(t)$ | $=$ | $\beta\lambda(t-1) + \lvert y(t)\rvert^2$ |
| $\mathbf{a}(t)$ | $=$ | $\mathbf{a}(t-1) + [\mathbf{z}(t) - \mathbf{a}(t-1)y(t)]\, y(t)^* / \lambda(t)$ |

where $y(i) \stackrel{\Delta}{=} \boldsymbol{a}_1(i-1)^H \boldsymbol{z}_1(i)$, is the approximation of the unknown projection $\boldsymbol{a}_1(t)^H \boldsymbol{z}_1(i)$ of $\boldsymbol{z}_1(i)$ onto $\boldsymbol{a}_1(t)$. Then by minimizing $\tilde{\mathcal{L}}[\boldsymbol{a}_1(t)]$ in (62) recursively, a blind adaptive algorithm for array response estimation is obtained. This algorithm is listed in Table II.

*Example 4:* This example illustrates the performance of the blind adaptive array response estimation algorithm. Consider an array of $J = 3$ sensors, with half-wavelength spacing, i.e., $d = \lambda/2$. The DOA of the signal of interest varies according to $\theta_1 = (\pi/3) \cdot (t/1000) - (\pi/6)$, for $0 \le t \le 1000$. Then by (57) the phases of the first and third sensor response satisfy $\phi_{11} = -\phi_{13} = (\pi/1000) \cdot t - (\pi/2)$, for $0 \le t \le 1000$. Shown in Fig. 5 are plots of the estimated phases of the array response, based on the output of the bank of (exact) decorrelators (Fig. 5(a)) and the output of the bank of subspace-based adaptive MMSE detectors (Fig 5(b)). It is seen that the proposed algorithm can closely track the array response to the signal of interest.

## VII. CONCLUSION

In this paper, we have developed a new blind adaptive multiuser detection technique based on signal subspace estimation. Compared with the previous minimum-output-energy blind adaptive multiuser detection algorithm, it is seen that the proposed method has lower computational complexity and better performance, and it is robust against signature waveform mismatch. Within the framework of signal subspace estimation, we have also developed a blind adaptive algorithm for estimating the effective signature waveform in the multipath channel, and a blind adaptive algorithm for estimating the array response when an antenna array is employed. It is seen that under the proposed subspace approach, blind adaptive channel estimation and blind adaptive array response estimation can be integrated with blind adaptive multiuser detection, with little attendant increase in complexity. Finally, we note from the simulation examples that the PASTd subspace tracking algorithm has a relatively slow convergence rate, which may pose a problem for a time-varying system. Nevertheless, subspace tracking is a very active research field in signal processing and it is anticipated that with the emergence of more powerful fast subspace trackers (e.g., [30]), the performance of the subspace-based adaptive multiuser detectors will be improved.

## APPENDIX I
## PROOF OF LEMMA 3

Denote $\boldsymbol{H} \stackrel{\Delta}{=} \boldsymbol{SAS}^T$ and $\boldsymbol{G} \stackrel{\Delta}{=} \boldsymbol{W}\boldsymbol{\Sigma}^{\dagger T}\boldsymbol{V}^T\boldsymbol{A}^{-1}\boldsymbol{V}\boldsymbol{\Sigma}^{\dagger}\boldsymbol{W}^T$. From (8), the eigenvalue decomposition of $\boldsymbol{H}$ is given by $\boldsymbol{H} \stackrel{\Delta}{=} \boldsymbol{SAS}^T = \boldsymbol{U}\boldsymbol{\Lambda}_0\boldsymbol{U}^T$. Then the Moore–Penrose generalized

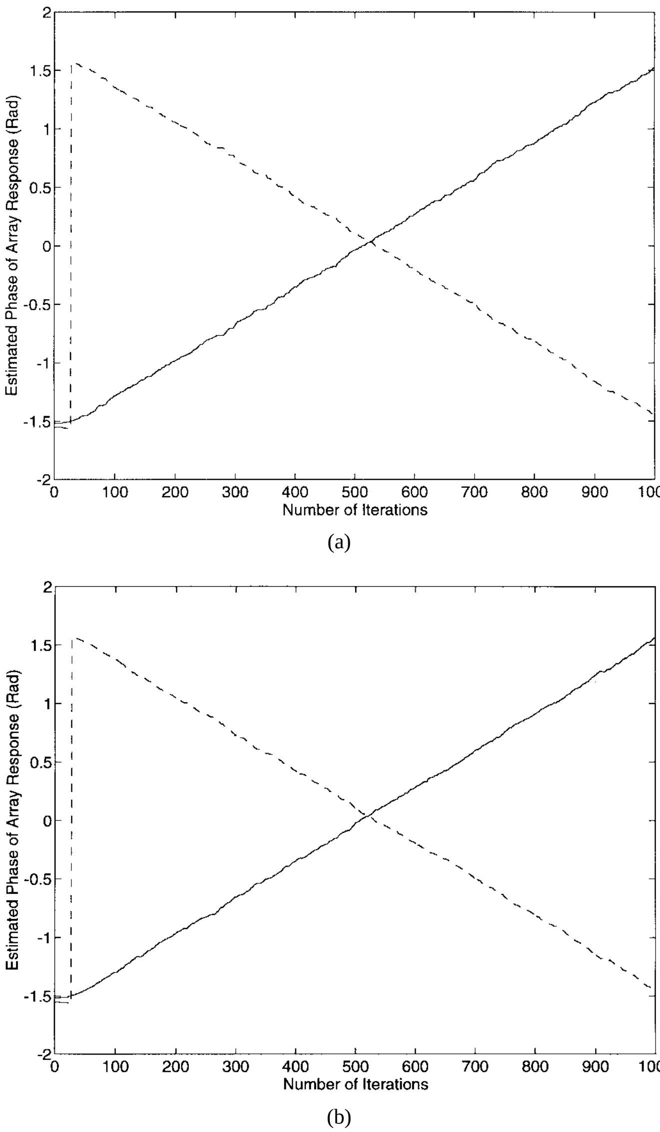


Fig. 5. Performance of the blind adaptive algorithm for array response estimation. The number of sensors $J = 3$, with half-wavelength spacing, i.e., $d = \lambda/2$. The DOA of the signal of interest $\theta_1$ varies with time such that the phases of the sensor responses $\phi_1$ varies linearly from $-(\pi/2)$ to $\pi/2$, and $\phi_3$ varies linearly from $\pi/2$ to $-(\pi/2)$. Shown are the plots of the estimated phases of the array response. In (a) the estimation is based on the outputs of the exact decorrelating detectors. In (b) the estimation is based on the outputs of the subspace-based blind adaptive MMSE detectors. The forgetting factor used in the array response estimation algorithm is $0.96$ and that in the subspace tracking algorithm is $0.995$. It is seen that in both plots the array response is closely tracked.

inverse [11] of matrix $\boldsymbol{H}$ is given by

$$\boldsymbol{H}^\dagger = (\boldsymbol{SAS}^T)^\dagger = \boldsymbol{U}\boldsymbol{\Lambda}_0^\dagger \boldsymbol{U}^T. \tag{63}$$

On the other hand, the Moore–Penrose generalized inverse $\boldsymbol{H}^\dagger$ of a matrix $\boldsymbol{H}$ is the unique matrix that satisfies [11] a) $\boldsymbol{HH}^\dagger$ and $\boldsymbol{H}^\dagger\boldsymbol{H}$ are symmetric; b) $\boldsymbol{HH}^\dagger\boldsymbol{H} = \boldsymbol{H}$; and c) $\boldsymbol{H}^\dagger\boldsymbol{HH}^\dagger = \boldsymbol{H}^\dagger$. Next we show that $\boldsymbol{G} = \boldsymbol{H}^\dagger$ by verifying these three conditions. We first verify condition a). Using (25), we have

$$\begin{aligned}\boldsymbol{HG} &= (\boldsymbol{W\Sigma V}^T\boldsymbol{AV\Sigma}^T\boldsymbol{W}^T)(\boldsymbol{W\Sigma}^{\dagger T}\boldsymbol{V}^T\boldsymbol{A}^{-1}\boldsymbol{V\Sigma}^\dagger\boldsymbol{W}^T)\\ &= \boldsymbol{W\Sigma\Sigma}^\dagger\boldsymbol{W}^T\end{aligned} \tag{64}$$

where the second equality follows from the facts that $\boldsymbol{W}^T\boldsymbol{W} = \boldsymbol{I}_N$ and $\boldsymbol{\Sigma}^T\boldsymbol{\Sigma}^{\dagger T} = \boldsymbol{V}^T\boldsymbol{V} = \boldsymbol{VV}^T = \boldsymbol{I}_K$. Since the $N \times N$ diagonal matrix $\boldsymbol{\Sigma\Sigma}^\dagger = \mathrm{diag}\,(\boldsymbol{I}_k, \boldsymbol{0})$, it follows from (64) that $\boldsymbol{HG}$ is symmetric. Similarly, $\boldsymbol{GH}$ is also symmetric. Next we verify condition b).

$$\begin{aligned}\boldsymbol{HGH} &= (\boldsymbol{W\Sigma V}^T\boldsymbol{AV\Sigma}^T\boldsymbol{W}^T)(\boldsymbol{W\Sigma}^{\dagger T}\boldsymbol{V}^T\boldsymbol{A}^{-1}\boldsymbol{V\Sigma}^\dagger\boldsymbol{W}^T)\\ &\quad\cdot(\boldsymbol{W\Sigma V}^T\boldsymbol{AV\Sigma}^T\boldsymbol{W}^T)\\ &= \boldsymbol{W\Sigma\Sigma}^\dagger\boldsymbol{\Sigma V}^T\boldsymbol{AV\Sigma}^T\boldsymbol{W}^T\\ &= \boldsymbol{W\Sigma V}^T\boldsymbol{AV\Sigma}^T\boldsymbol{W}^T\\ &= \boldsymbol{SAS}^T = \boldsymbol{H}\end{aligned} \tag{65}$$

where in the second equality, the following facts are used: $\boldsymbol{W}^T\boldsymbol{W} = \boldsymbol{I}_N$, $\boldsymbol{\Sigma}^T\boldsymbol{\Sigma}^{\dagger T} = \boldsymbol{I}_K$, and $\boldsymbol{V}^T\boldsymbol{V} = \boldsymbol{VV}^T = \boldsymbol{I}_K$; the third equality follows from the fact that $\boldsymbol{\Sigma\Sigma}^\dagger\boldsymbol{\Sigma} = \boldsymbol{\Sigma}$. Condition c) can be similarly verified, i.e., $\boldsymbol{GHG} = \boldsymbol{G}$. Therefore, we have

$$\boldsymbol{U\Lambda}_0^\dagger\boldsymbol{U}^T = \boldsymbol{H}^\dagger = \boldsymbol{G} = \boldsymbol{W\Sigma}^{\dagger T}\boldsymbol{V}^T\boldsymbol{A}^{-1}\boldsymbol{V\Sigma}^\dagger\boldsymbol{W}^T. \tag{66}$$

Now (26) follows immediately from (66) and the fact that $\boldsymbol{U}^T\boldsymbol{U} = \boldsymbol{UU}^T = \boldsymbol{I}_N$. □

## Appendix II
## Proof of Lemma 4

Define

$$\boldsymbol{d} \triangleq \boldsymbol{U}_s(\boldsymbol{\Lambda}_s - \sigma^2\boldsymbol{I}_K)^{-1}\boldsymbol{U}_s^T\boldsymbol{s}_1 = \boldsymbol{U\Lambda}_0^\dagger\boldsymbol{U}^T\boldsymbol{s}_1.$$

Then from (13) we have $\boldsymbol{d}_1 = \boldsymbol{d}/(\boldsymbol{d}^T\boldsymbol{s}_1)$. Let $\boldsymbol{e}_k$ be the $k$th unit basis of $\mathcal{R}^K$, i.e., all entries of $\boldsymbol{e}_k$ are zeros except the $k$th entry, which is 1. Since $\boldsymbol{s}_k = \boldsymbol{Se}_k$, we have

$$\begin{aligned}\boldsymbol{d}^T\boldsymbol{s}_k &= \boldsymbol{s}_1^T\boldsymbol{U\Lambda}_0^\dagger\boldsymbol{U}^T\boldsymbol{Se}_k^T\\ &= \boldsymbol{e}_1^T\boldsymbol{S}^T(\boldsymbol{SAS})^\dagger\boldsymbol{Se}_k^T\\ &= \boldsymbol{e}_1^T(\boldsymbol{V\Sigma}^T\boldsymbol{W}^T)(\boldsymbol{W\Sigma}^{\dagger T}\boldsymbol{V}^T\boldsymbol{A}^{-1}\boldsymbol{V\Sigma}^\dagger\boldsymbol{W}^T)(\boldsymbol{W\Sigma V}^T)\boldsymbol{e}_k\\ &= \boldsymbol{e}_1^T\boldsymbol{A}^{-1}\boldsymbol{e}_k = \begin{cases} A_1^{-2}, & k=1\\ 0, & k = 2,\cdots,K\end{cases}\end{aligned} \tag{67}$$

where the second equality follows from (63); the third equality follows from (25) and (66); and the fourth equality follows from the facts that $\boldsymbol{W}^T\boldsymbol{W} = \boldsymbol{I}_N$, $\boldsymbol{\Sigma}^T\boldsymbol{\Sigma}^{\dagger T} = \boldsymbol{\Sigma}^\dagger\boldsymbol{\Sigma} = \boldsymbol{I}_K$, and $\boldsymbol{VV}^T = \boldsymbol{I}_K$. Therefore, $\boldsymbol{d}_1^T\boldsymbol{s}_1 = 1$, and $\boldsymbol{d}_1^T\boldsymbol{s}_k = 0$, for $k = 2,\cdots,K$.

To prove (29), using (67), we notice that

$$\boldsymbol{d}_1^T\boldsymbol{d}_1 = (\boldsymbol{d}^T\boldsymbol{d})/(\boldsymbol{d}^T\boldsymbol{s}_1)^2 = A_1^4\boldsymbol{d}^T\boldsymbol{d} \tag{68}$$

where

$$\begin{aligned}\boldsymbol{d}^T\boldsymbol{d} &= \boldsymbol{s}_1^T\boldsymbol{U\Lambda}_0^\dagger\boldsymbol{U}^T\boldsymbol{U\Lambda}_0^\dagger\boldsymbol{U}^T\boldsymbol{s}_1^T\\ &= \boldsymbol{e}_1^T(\boldsymbol{V\Sigma}^T\boldsymbol{W}^T)\boldsymbol{U\Lambda}_0^\dagger\boldsymbol{\Lambda}_0^\dagger\boldsymbol{U}^T(\boldsymbol{W\Sigma V}^T)\boldsymbol{e}_1\\ &= \boldsymbol{e}_1^T(\boldsymbol{V\Sigma}^T\boldsymbol{W}^T)\boldsymbol{U}(\boldsymbol{U}^T\boldsymbol{W\Sigma}^{\dagger T}\boldsymbol{V}^T\boldsymbol{A}^{-1}\boldsymbol{V\Sigma}^\dagger\boldsymbol{W}^T\boldsymbol{U})\\ &\quad\cdot(\boldsymbol{U}^T\boldsymbol{W\Sigma}^{\dagger T}\boldsymbol{V}^T\boldsymbol{A}^{-1}\boldsymbol{V\Sigma}^\dagger\boldsymbol{W}^T\boldsymbol{U})\boldsymbol{U}^T(\boldsymbol{W\Sigma V}^T)\boldsymbol{e}_1\\ &= \boldsymbol{e}_1^T\boldsymbol{A}^{-1}[\boldsymbol{V}(\boldsymbol{\Sigma}^\dagger\boldsymbol{\Sigma}^{\dagger T})\boldsymbol{V}^T]\boldsymbol{A}^{-1}\boldsymbol{e}_1\\ &= A_1^{-4}\boldsymbol{e}_1^T[\boldsymbol{V}(\boldsymbol{\Sigma}^T\boldsymbol{\Sigma})^{-1}\boldsymbol{V}^T]\boldsymbol{e}_1\\ &= A_1^{-4}\boldsymbol{e}_1^T(\boldsymbol{S}^T\boldsymbol{S})^{-1}\boldsymbol{e}_1 = A_1^{-4}[\boldsymbol{R}^{-1}]_{11}\end{aligned} \tag{69}$$

where the second equality follows from the facts that $\boldsymbol{U}^T\boldsymbol{U} = \boldsymbol{I}_N$, $\boldsymbol{s}_1 = \boldsymbol{S}\boldsymbol{e}_1$, and (25); the third equality follows from (26); the fourth equality follows from the facts that $\boldsymbol{U}\boldsymbol{U}^T = \boldsymbol{W}^T\boldsymbol{W} = \boldsymbol{I}_N$ and $\boldsymbol{\Sigma}^T\boldsymbol{\Sigma}^{\dagger T} = \boldsymbol{\Sigma}^\dagger\boldsymbol{\Sigma} = \boldsymbol{V}\boldsymbol{V}^T = \boldsymbol{I}_K$; the sixth equality follows from (25); and the last equality follows from the fact that $\boldsymbol{R} = \boldsymbol{S}^T\boldsymbol{S}$. □

## Appendix III
## Proof of Proposition 6

Define $\boldsymbol{B} \triangleq \boldsymbol{D}^H\boldsymbol{D}$. The proof in [19] is only for a real symmetric matrix $\boldsymbol{B}$. In the following we give a proof for a Hermitian matrix $\boldsymbol{B}$. Since $\boldsymbol{B}$ is Hermitian we have $\boldsymbol{B}_R^T = \boldsymbol{B}_R$ and $\boldsymbol{B}_I^T = -\boldsymbol{B}_I$, where the subscript $_R$ and $_I$ represent the real and imaginary parts of the complex matrix, respectively. Now define $\underline{\mathrm{x}} \triangleq [\boldsymbol{x}_R^T \; \boldsymbol{x}_I^T]^T$ and $\underline{\mathrm{B}} \triangleq \begin{bmatrix} \boldsymbol{B}_R & -\boldsymbol{B}_I \\ \boldsymbol{B}_I & \boldsymbol{B}_R \end{bmatrix}$. Then it can be readily verified that $q(\boldsymbol{x}, c)$ in (55) can be written as

$$q(\boldsymbol{x}, c) = \frac{1}{2}\, \underline{\mathrm{x}}^T \underline{\mathrm{B}}\, \underline{\mathrm{x}} + \frac{c}{4}\, (\underline{\mathrm{x}}^T \underline{\mathrm{x}} - 1)^2. \tag{70}$$

The gradient and Hessian matrix of $q(\boldsymbol{x}, c)$ are given, respectively, by

$$\nabla q(\boldsymbol{x}, c) = \underline{\mathrm{B}}\, \underline{\mathrm{x}} + c(\underline{\mathrm{x}}^T\underline{\mathrm{x}} - 1)\underline{\mathrm{x}} \tag{71}$$
$$\nabla^2 q(\boldsymbol{x}, c) = \underline{\mathrm{B}} + c(\underline{\mathrm{x}}^T\underline{\mathrm{x}} - 1)\boldsymbol{I} + 2c\,\underline{\mathrm{x}}\,\underline{\mathrm{x}}^T. \tag{72}$$

Let $\nu_1, \cdots, \nu_{K+L}$ and $\boldsymbol{v}_1, \cdots, \boldsymbol{v}_{K+L}$ be the eigenvalues and corresponding eigenvectors of the matrix $\boldsymbol{B}$. It can be verified that each $\nu_i$ is an eigenvalue of $\underline{\mathrm{B}}$ of multiplicity 2, with the corresponding eigenvectors $\underline{\mathrm{v}}_k \triangleq [\boldsymbol{v}_{i_R}^T \; \boldsymbol{v}_{i_I}^T]^T$ and $\underline{\mathrm{v}}'_k \triangleq [-\boldsymbol{v}_{i_I}^T \; \boldsymbol{v}_{i_R}^T]^T$. It is then seen from (71) that $\nabla q(\boldsymbol{x}, c) = \boldsymbol{0}$ if and only if $\underline{\mathrm{x}}$ is a scaled version of an eigenvector of matrix $\underline{\mathrm{B}}$, or equivalently, $\boldsymbol{x}$ is a scaled version of matrix $\boldsymbol{B}$, i.e., $\boldsymbol{x} = \|\boldsymbol{x}\|\boldsymbol{v}_k$. The norm $\|\boldsymbol{x}\|$ is determined from

$$\begin{aligned} \boldsymbol{0} = \nabla q(\|\boldsymbol{x}\|\boldsymbol{v}_k, c) &= \underline{\mathrm{B}}\|\boldsymbol{x}\|\underline{\mathrm{v}}_k + c(\|\boldsymbol{x}\|^2 - 1)\|\boldsymbol{x}\|\underline{\mathrm{v}}_k \\ &= \nu_k\|\boldsymbol{x}\|\underline{\mathrm{v}}_k + c(\|\boldsymbol{x}\|^2 - 1)\|\boldsymbol{x}\|\underline{\mathrm{v}}_k. \end{aligned} \tag{73}$$

Solving for $\|\boldsymbol{x}\|$ we obtain $\|\boldsymbol{x}\| = \sqrt{1 - (\nu_k/c)}$. Now the Hessian matrix at any stationary point $\boldsymbol{x} = \sqrt{1 - (\nu_k/c)}\boldsymbol{v}_k$ is

$$\begin{aligned} \nabla^2 q\left(\sqrt{1 - \frac{\nu_k}{c}}\, \boldsymbol{v}_k, c\right) &= \underline{\mathrm{B}} - \nu_k\boldsymbol{I} + 2(c - \nu_k)\underline{\mathrm{v}}_k\underline{\mathrm{v}}_k^T \\ &= \boldsymbol{V}\boldsymbol{\Phi}\boldsymbol{V}^T \end{aligned} \tag{74}$$

where $\boldsymbol{V} \triangleq [\underline{\mathrm{v}}_1 \; \underline{\mathrm{v}}'_1 \cdots \underline{\mathrm{v}}_{K+L} \; \underline{\mathrm{v}}'_{K+L}]$ and $\boldsymbol{\Phi} \triangleq \mathrm{diag}\,(\nu_1 - \nu_k, \nu_1 - \nu_k, \cdots, \nu_{k-1} - \nu_k, \nu_{k-1} - \nu_k, 2(c - \nu_k), 2(c - \nu_k), \nu_{k+1} - \nu_k, \nu_{k+1} - \nu_k, \cdots, \nu_{K+L} - \nu_k, \nu_{K+L} - \nu_k)$. It is seen from (74) that the Hessian is semipositive definite if and only if $\nu_k$ is the smallest eigenvalue of the matrix $\boldsymbol{B}$, then the corresponding stationary point is the only local minimum; otherwise, the Hessian is indefinite at the stationary point, which is a saddle point. On the other hand,

$$\begin{aligned} q(\boldsymbol{x}, c) &\geq \frac{1}{2}\, \nu_{\min}\boldsymbol{x}^H\boldsymbol{x} + \frac{c}{4}\, (\boldsymbol{x}^H\boldsymbol{x} - 1)^2 \\ &= \frac{c}{4}\left[\boldsymbol{x}^H\boldsymbol{x} - \left(1 - \frac{\nu_{\min}}{c}\right)\right]^2 \\ &\quad + \left(\frac{\nu_{\min}}{2} - \frac{\nu_{\min}^2}{4c}\right) \end{aligned} \tag{75}$$

with equality achieved if and only if $\boldsymbol{x}$ is a scaled version of the minimum eigenvector with norm $\|\boldsymbol{x}\| = \sqrt{1 - (\nu_{\min}/c)}$. Therefore, the local minimum is the global minimum. □

## References


[1] A. Abdulrahman, D. D. Falconer, and A. U. Sheikh, "Decision feedback equalization for CDMA in indoor wireless communications," *IEEE J. Select. Areas Commun.*, vol. 12, pp. 698–706, May 1994.

[2] S. E. Bensley and B. Aazhang, "Subspace-based channel estimation for code-division multiple-access communication systems," *IEEE Trans. Commun.*, vol. 44, pp. 1009–1020, Aug. 1996.

[3] C. H. Bischof and G. M. Shroff, "On updating signal subspaces," *IEEE Trans. Signal Processing*, vol. 40, pp. 96–105, Jan. 1992.

[4] D.-S. Chen and S. Roy, "An adaptive multiuser receiver for CDMA systems," *IEEE J. Select. Areas Commun.*, vol. 12, pp. 808–816, June 1994.

[5] P. Comon and G. H. Golub, "Tracking a few extreme singular values and vectors in signal processing," *Proc. IEEE*, vol. 78, pp. 1327–1343, Aug. 1990.

[6] R. D. DeGroat, "Noniterative subspace tracking," *IEEE Trans. Signal Processing*, vol. 40, pp. 571–577, Mar. 1992.

[7] M. Honig, U. Madhow, and S. Verdú, "Blind multiuser detection," *IEEE Trans. Inform. Theory*, vol. 41, pp. 944–960, July 1995.

[8] M. Honig and H. V. Poor, "Adaptive interference suppression in wireless communication systems," in H. V. Poor and G. W. Wornell, Eds., *Wireless Communications: Signal Processing Perspectives*. Upper Saddle River, NJ: Prentice Hall, 1998.

[9] M. L. Honig, "Adaptive linear interference suppression for packet DS-CDMA," *European Trans. Telecomm.* (Special Issue on CDMA), 1997.

[10] ——, "A comparison of subspace adaptive filtering techniques for DS-CDMA interference suppression," in *Proc. 1997 Milcom*, 1997.

[11] R. A. Horn and C. R. Johnson, *Matrix Analysis*. London, U.K.: Cambridge Univ. Press, 1985.

[12] H. C. Huang, S. Schwartz, and S. Verdú, "Combined multipath and spatial resolution for multiuser detecion: Potentials and problems," in *Proc. 1995 IEEE Int. Symp. on Information Theory* (Whistler, BC, Canada, Sept. 1995), p. 205.

[13] R. Kohno, R. Meidan, and L. Milstein, "Spread spectrum access method for wireless communications," *IEEE Commun. Mag.*, pp. 58–67, Jan. 1995.

[14] H. Liu and G. Xu, "A subspace method for signal waveform estimation in synchronous CDMA systems," *IEEE Trans. Commun.*, vol. 44, pp. 1346–1354, Oct. 1996.

[15] D. G. Luenberger, *Linear and Nonlinear Programming*, 2nd ed. Reading, MA: Addision-Wesley, 1989.

[16] R. Lupas and S. Verdú, "Linear multi-user detectors for synchronous code-division multiple-access channels," *IEEE Trans. Inform. Theory*, vol. 35, pp. 123–136, Jan. 1989.

[17] U. Madhow and M. Honig, "MMSE interference suppression for direct-sequence spread-spectrum CDMA," *IEEE Trans. Commun.*, vol. 42, pp. 3178–3188, Dec. 1994.

[18] R. K. Madyastha and B. Aazhang, "Multiuser receivers for cdma communication systems using antenna arrays," in *Proc. 32th Annu. Allerton Conf. on Communications, Computing and Control* (Monticello, IL, Oct. 1994).

[19] G. Mathew and V. U. Reddy, "Development and analysis of a neural network approach to Pisarenko's harmonic retrieval method," *IEEE Trans. Signal Processing*, vol. 42, pp. 663–667, Mar. 1994.

[20] S. L. Miller, "An adaptive direct-sequence code-division multiple-access receiver for multiuser interference rejection," *IEEE Trans. Commun.*, vol. 43, pp. 1556–1565, Feb./Mar./Apr. 1995.

[21] U. Mitra and H. V. Poor, "Adaptive receiver algorithms for near-far resistant CDMA," *IEEE Trans. Commun.*, vol. 43, pp. 1713–1724, 1995.

[22] ——, "Analysis of an adaptive decorrelating detector for synchronous CDMA channels," *IEEE Trans. Commun.*, vol. 44, Feb. 1996.

[23] A. F. Naguib, A. Paulraj, and T. Kailath, "Capacity improvement with base-station antenna arrays in cellular CDMA," *IEEE Trans. Veh. Technol.*, vol. 43, pp. 691–698, Mar. 1994.

[24] H. V. Poor and S. Verdú, "Probability of error in MMSE multiuser detection," *IEEE Trans. Inform. Theory*, vol. 43, pp. 858–871, May 1997.

[25] H. V. Poor, *An Introduction to Signal Detection and Estimation*, 2nd ed. New York: Springer-Verlag, 1994.

[26] H. V. Poor and X. Wang, "Code-aided interference suppression in DS/CDMA communications—Part II: Parallel blind adaptive implementations," *IEEE Trans. Commun.*, vol. 45, pp. 1112–1122, Sept. 1997.

[27] J. G. Proakis, *Digital Communications*, 3rd ed. New York: McGraw-Hill, 1995.
[28] P. B. Rapajic and B. S. Vucetic, "Adaptive receiver structures for asynchronous CDMA systems," *IEEE J. Select. Areas Commun.*, vol. 12, pp. 685–697, May 1994.
[29] G. W. Stewart, "An updating algorithm for subspace tracking," *IEEE Trans. Signal Processing*, vol. 40, pp. 1535–1541, June 1992.
[30] P. Strobach, "Low-rank adaptive filters," *IEEE Trans. Signal Processing*, vol. 44, pp. 2932–2947, Dec. 1996.
[31] E. G. Strom, S. Parkvall, S. L. Miller, and B. E. Ottersten, "Propagation delay estimation in asynchronous direct-sequence code-division multiple access systems," *IEEE Trans. Commun.*, vol. 44, pp. 84–93, Jan. 1996.
[32] V. G. Subramanian and U. Madhow, "Blind demodulation of direct-sequence CDMA signals using an antenna array," in *Proc. 1996 Conf. on Information Science and Systems*, 1996.
[33] D. W. Tufts and C. D. Melissinos, "Simple, effective computation of principle eignevectors and their eigenvalues and application to high resolution estimation of frequencies," *IEEE Trans. Acoust. Speech. Signal Processing*, vol. 34, pp. 1046–1053, Oct. 1986.
[34] A. van der Veen, E. Deprettere, and A. Swindlehurst, "Subspace-based signal analysis using singular value decomposition," *Proc. IEEE*, vol. 81, pp. 1277–1308, Sept. 1993.
[35] S. Verdú, *Multiuser Detection*. Cambridge, UK: Cambridge Univ. Press, 1998.
[36] M. Viberg and B. Ottersten, "Sensor array processing based on subspace fitting," *IEEE Trans. Signal Processing*, vol. 39, pp. 1110–1120, May 1991.
[37] A. J. Viterbi, "The orthogonal-random wave form dichotomy for digital mobile personal communications," *IEEE Personal Commun. Mag.*, vol. 1, pp. 18–24, Feb. 1994.
[38] X. Wang and H. V. Poor, "Blind equalization and multiuser detection for cdma communications in dispersive channels," *IEEE Trans. Commun.*, vol. 46, pp. 91–103, Jan. 1998.
[39] M. Wax and T. Kailath, "Detection of signals by information theoretic criteria," *IEEE Trans. Acoust. Speech. Signal Processing*, vol. ASSP-33, pp. 387–392, Apr. 1985.
[40] B. Yang, "An extension of the PASTd algorithm to both rank and subspace tracking," *IEEE Signal Processing Let.*, vol. 2, pp. 179–182, Sept. 1995.
[41] ——, "Projection approximation subspace tracking," *IEEE Trans. Signal Processing*, vol. 44, pp. 95–107, Jan. 1995.
[42] ——, "Asymptotic convergence analysis of the projection approximation subspace tracking algorithms," *Signal Processing*, vol. 50, pp. 123–136, 1996.
[43] L. C. Zhao, P. R. Krishnaiah, and Z. D. Bai, "On detection of the number of signals in the presence of white nosie," *J. Multivar. Anal.*, pp. 1–25, 1986.